Conclusions

The use of trapped-mode resonators in microwave band-pass filters was demonstrated to provide a means for obtaining a prescribed pass band, with very broad stop bands. It appears that by redesigning the conventional resonators at the ends of the filter so as to make their cavity proportions more dissimilar, the resonances in the conventional resonators could be further separated in frequency, and as a result the minimum stop band attenuation could be maintained at an even higher level. Although this point has not been investigated, it is probable that the power-handling ability of filters of this type will be the same as that for conventional filters using circular TE_{011}-mode resonators [13].

Acknowledgment

The trial trapped-mode filter was constructed by C. A. Knight and R. Pierce. The laboratory tests were performed by Y. Sato.

References

[1] B. M. Schiffman, G. L. Matthaei, and L. Young, "A rectangular-waveguide filter using trapped-mode resonators," this issue, pp. 000–000.
[2] V. Met, "Absorptive filters for microwave harmonic power," *Proc. IRE*, vol. 47, pp. 1762–1769, October 1959.
[3] H. G. Unger, "Normal modes and mode conversion in helix waveguide," *Bell Sys. Tech. J.*, vol. 60, pp. 255–280, January 1961.
[4] E. L. Ginzton, *Microwave Measurements*. New York: McGraw-Hill, 1957, pp. 355, 366.
[5] N. Marcuvitz, *Waveguide Handbook*, MIT Rad. Lab. Ser., vol. 10, New York: McGraw-Hill, 1951, pp. 195, 196, 291.
[6] E. G. Cristal, G. L. Matthaei, and D. B. Weller, "Novel microwave filter design techniques," Stanford Research Institute, Menlo Park, Calif., Quart. Prog. Rept. 3, SRI Project 4344, Contract DA 36-039 AM-00084(E), sec. 4, September 1963.
[7] D. A. Lanciani, "H_{01}-mode circular waveguide components," *IRE Trans. on Microwave Theory and Techniques*, vol. MTT-2, pp. 45–51, July 1954.
[8] S. B. Cohn, "Dissipation loss in multiple-coupled-resonator filters," *Proc. IRE*, vol. 47, pp. 1342–1348, August 1959.
[9] G. L. Matthaei, L. Young, and E. M. T. Jones, *Microwave Filters, Impedance-Matching Networks, and Coupling Structures*, sec. 11.06. New York: McGraw-Hill, 1964.
[10] *Ibid.*, secs. 11.02–11.04.
[11] *Ibid.*, sec. 8.02.
[12] M. Dishal, "Alignment and adjustment of synchronously tuned multiple-resonator-circuit filters," *Proc. IRE*, vol. 39, pp. 1448–1455, November 1951.
[13] G. L. Matthaei, L. Young, and E. M. T. Jones [9], sec. 15.04.

Design of Band-Stop Filters in the Presence of Dissipation

J. J. TAUB, SENIOR MEMBER, IEEE, AND R. L. SLEVEN, MEMBER, IEEE

***Abstract*—The insertion loss vs. frequency characteristic of equal-element band-stop filters is derived for large as well as small degrees of dissipation, and for any number of resonators. These results are presented as curves for one through eight resonator filters.**

The equal-element band-stop filter, for small dissipation, is shown to have the lowest pass-band loss for a specified stop-band characteristic of all possible filters that can be represented by a low-pass prototype. Design procedures and examples are explained for waveguide and TEM band-stop filters. This includes selecting the optimum number of resonators, the resonator lengths, and the coupling reactances.

Experimental results on *C*-band waveguide and UHF coaxial filters are presented; the results are in good agreement with the theory. This approach makes possible complete prediction of the filter response and results in lower pass-band loss than could be obtained with previously used approaches.

I. Introduction

Design procedures available for microwave band-stop filters [1], [2] assume lossless circuit elements or consider dissipative effects as perturbations on lossless designs. In many narrow-band applications, these assumptions are not valid; techniques that include large, as well as small, dissipative effects in the design are desirable if close control of the response is to be obtained. This paper analyzes the equal-element (periodic) band-stop filter, allowing for lossy circuit elements. The equal-element response was selected because it minimizes dissipation loss in the pass band. An analysis using a lossy low-pass prototype is described. The insertion loss has been determined as a function of v (a normalized frequency variable), with u (a normalized dissipation factor) as a parameter, for any number of elements. These results are plotted for $n=1$ through 8 (with n the number of resonant circuits in each filter). These curves form the basis of a design procedure by which the required susceptance or reactance slope parameters can be determined. At this point in the procedure, the computation of resonator lengths and coupling geometry follows directly from a procedure given by Young et al. [1]. Examples of waveguide and coaxial filters designed according to this method agree closely with the theory presented.

Manuscript received September 8, 1964; revised January 25, 1965.
The authors are with the Airborne Instruments Laboratory, a Division of Cutler-Hammer, Inc., Deer Park, L. I., N. Y.

II. Equal-Element Band-Stop Filter Analysis

Low-Pass Prototype

The analysis is based on the transformation of the equivalent circuit of a band-stop filter to its low-pass prototype. Figure 1(a) shows the conventional low-pass prototype circuit, and Fig. 1(b) shows it modified to include dissipation. These prototypes can be analyzed to predict the behavior of band-stop filters by using the transformation

$$\frac{1}{\omega'} = \frac{1}{w\omega_1'}\left(\frac{\omega}{\omega_0} - \frac{\omega_0}{\omega}\right) \tag{1}$$

where

ω' = radian frequency of low-pass prototype
ω = radian frequency applied to band-stop filter
ω_0 = radian center frequency of band-stop filter.

The quantities ω_1' and w are defined in Figs. 1(c) and 2 for a specified band-edge attenuation. The series conductances G_1, G_3, $\cdots$ and shunt resistances R_2, R_4, $\cdots$ are expressed [3] as

$$G_1 = \frac{Q_{u_1}}{\omega_0 L_1} = w\omega_1' g_1 Q_{u_1}$$

$$R_2 = \frac{Q_{u_2}}{\omega_0 C_2} = w\omega_1' g_2 Q_{u_2} \tag{2}$$

where the values of Q_u are the unloaded Q's of the resonant circuits.

Equal-Element Filters

Although the circuit of Fig. 1(b) can be analyzed for any particular element values, we shall limit our discussion to the equal-element filter [3], [4]. By assuming uniform dissipation (all Q_u values equal), a group of insertion-loss functions for any value of n can be determined for large as well as small amounts of dissipation.

The equal-element type was chosen instead of Butterworth or Chebyshev designs because it has a lower dissipation loss in its pass band for a specified stop-band rejection. In Section III, it is shown that the equal-element filter has the lowest pass-band loss for a specified stop-band response of all possible designs having a fixed number of resonators; this property is valid for small dissipation loss. A similar property for the case of the equal-element band-pass filters was treated by Cohn [3]. Cohn showed that the equal-element band-pass filter, for small dissipation loss, has the lowest center-frequency loss for a specified stop-band rejection and number of resonators.

Insertion Loss vs. Frequency

The insertion loss vs. frequency is analyzed for equal-element band-stop filters in the Appendix. Expressions are obtained for any number of resonant circuits and are given specifically for $n=1$ through 8. The analysis assumes equal values of Q_u for all resonators and that the load resistor $g_{n+1}=g_0=1$.

The insertion-loss expressions are obtained by alternately multiplying the $ABCD$ matrices of the shunt and series elements of the lossy low-pass prototype. The insertion loss is obtained from the resultant $ABCD$ matrix terms, that is,

$$L = 10 \log \frac{|A_\tau + B_\tau + C_\tau + D_\tau|^2}{4}. \tag{3}$$

The loss expressions, as given in (37) in the Appendix, are functions of a single complex variable $X=u-jv$, where u is a normalized dissipation factor and v is a normalized frequency variable. From (32) and (33),

$$u = \frac{1}{w\omega_1' g Q_u} \tag{4}$$

$$v = \frac{1}{\omega' g}. \tag{5}$$

Curves of insertion loss vs. v (with u as a parameter) have been plotted in Figs. 3 through 18 for $n=1$ through 8. These data were obtained by programming (37) on a digital computer. The curves provide a map of possible equal-element band-stop filter responses for various dissipation factors. They therefore enable us to account for large as well as small dissipative losses in particular filter designs.

These curves enable us to determine the quantity $\omega_1'g$ by determining the required $v(v_1)$ corresponding to the start of the pass band for a known value of u. The value of $\omega_1'g$ is obtained from (5) and is equal to $1/v_1$. The required value of Q_u is obtained from (4) and is $Q_u=v_1/uw$. It is often desirable to use the fractional stop bandwidth w_s in the design equations rather than the fractional pass bandwidth w. In all equations v_s/w_s and v_1/w are interchangeable.

The reactance slope parameter of the shunt elements is

$$\frac{x}{Z_0} = \frac{\omega_0 L}{Z_0} = \frac{1}{w\omega_1' g} = \frac{v_1}{w} = \frac{v_s}{w_s}. \tag{6}$$

Similarly, the susceptance slope parameter b of the series elements is

$$\frac{b}{Y_0} = \frac{\omega_0 C}{Y_0} = \frac{1}{w\omega'_1 g} = \frac{v_1}{w} = \frac{v_s}{w_s} = \frac{x}{Z_0}. \tag{7}$$

The x and b parameters are important because they are directly related to the required coupling reactances and resonator lengths. The essential difference between the slope parameters determined here and those in reference [1] is that here x and b are modified from their lossless values by the v_1 term. Figures 19, 20, and 21 summarize the formulas used to obtain the coupling reactances and resonator lengths required for typical waveguide and TEM models. Section V explains their use in designing equal-element filters.

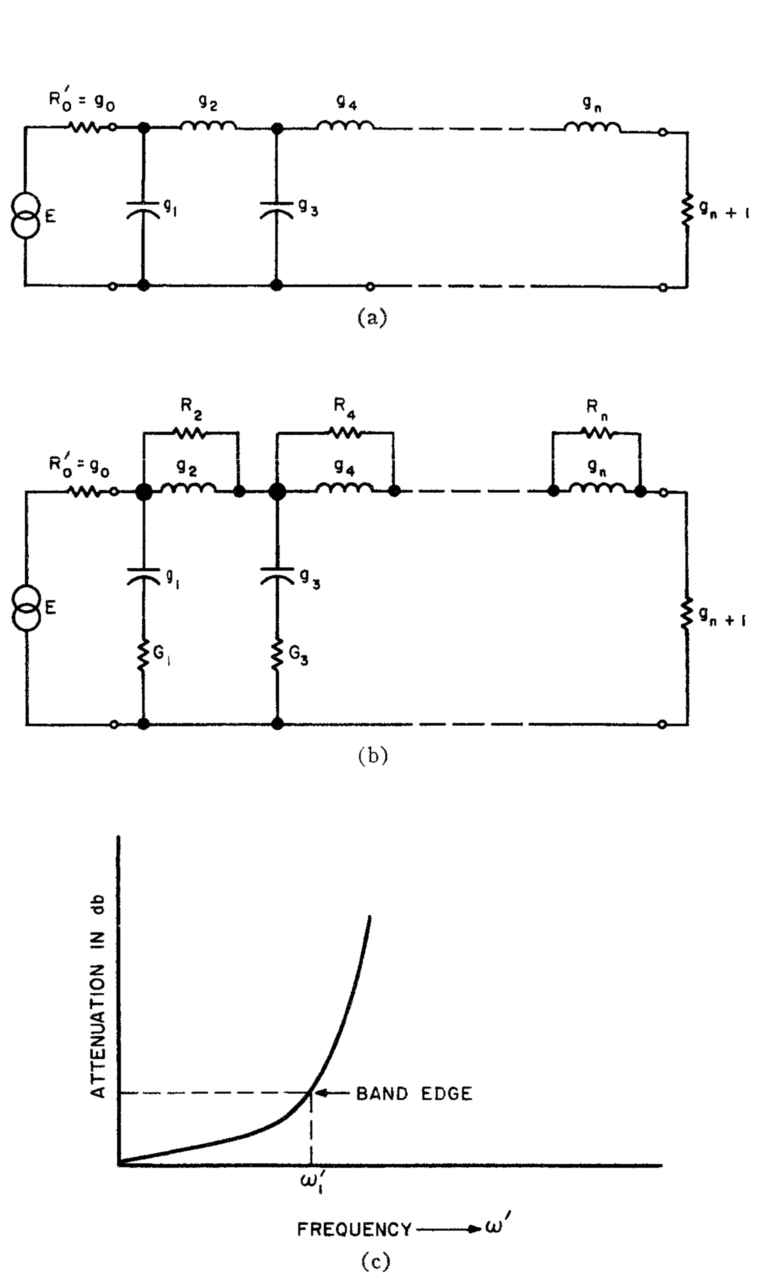

Fig. 1. (a) Low-pass prototype. (b) Dissipative low-pass prototype. (c) Low-pass filter characteristics.

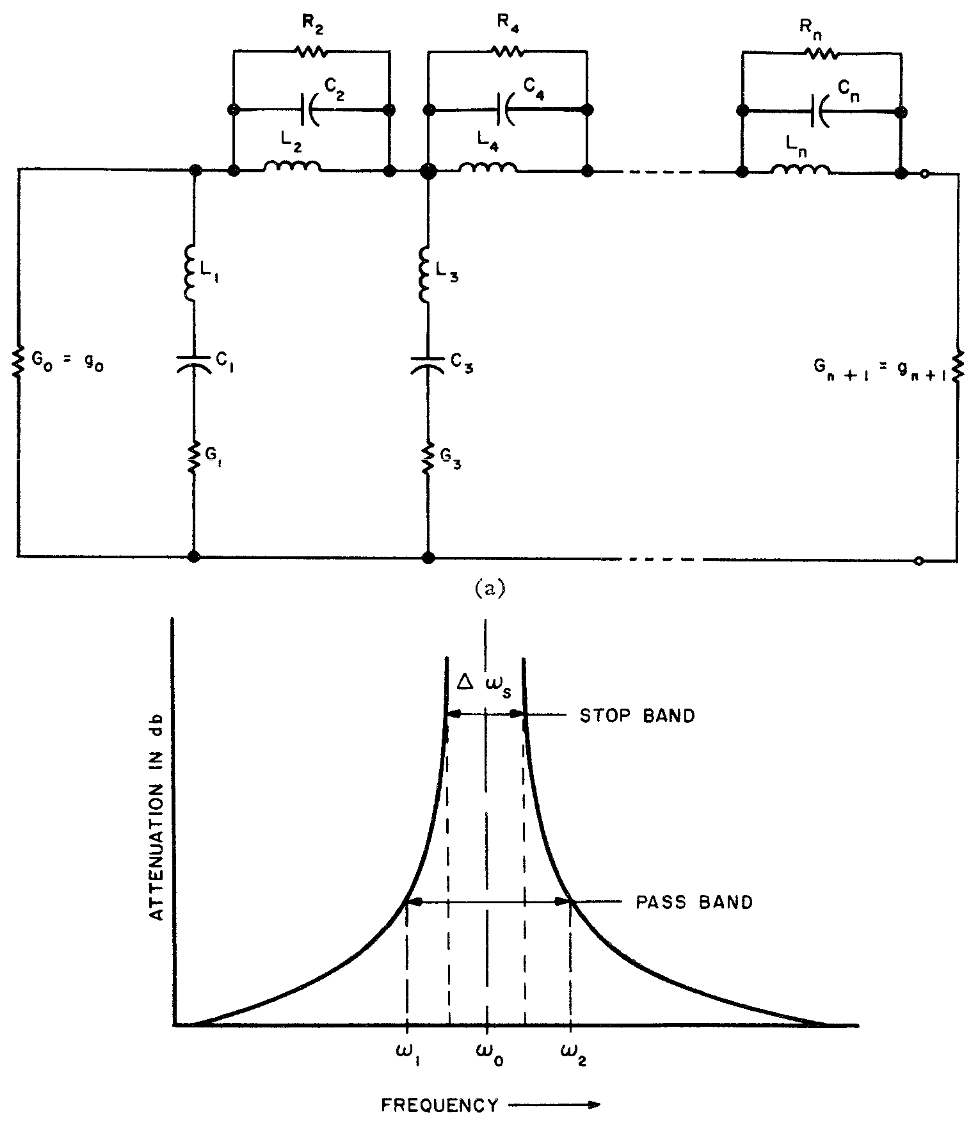

$$\omega_0 = \sqrt{\omega_1 \omega_2} \qquad W = \frac{\omega_2 - \omega_1}{\omega_0} \left(\frac{\lambda_g}{\lambda}\right)^2 \qquad W_s = \frac{\Delta \omega_s}{\omega_0} \left(\frac{\lambda_g}{\lambda}\right)^2$$

(b)

Fig. 2. (a) Band-stop filter derived from Fig. 1(b). (b) Band-stop filter characteristics.

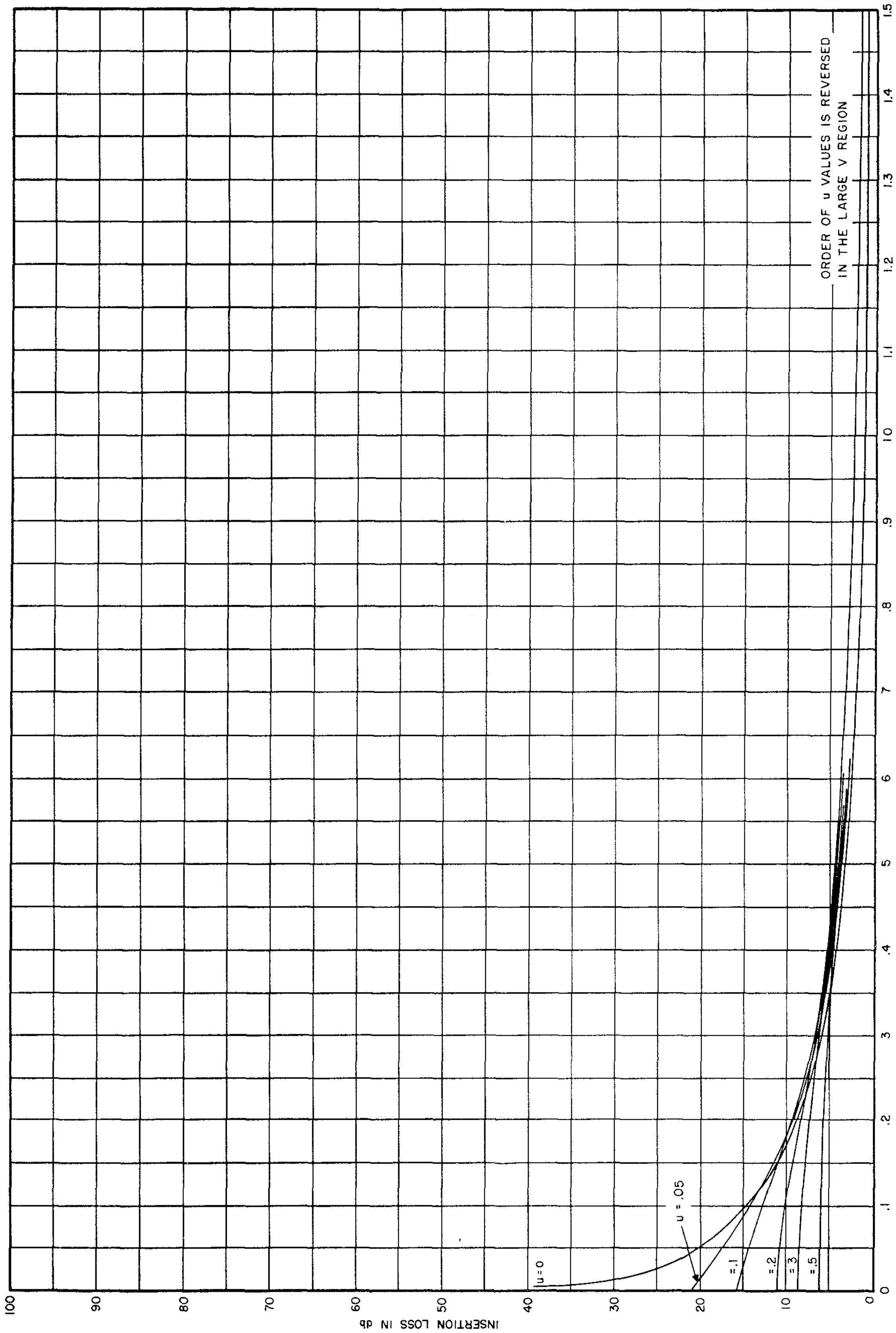

Fig. 3. Calculated stop-band insertion loss vs. normalized frequency with u as a parameter of dissipation ($n=1$ resonator).

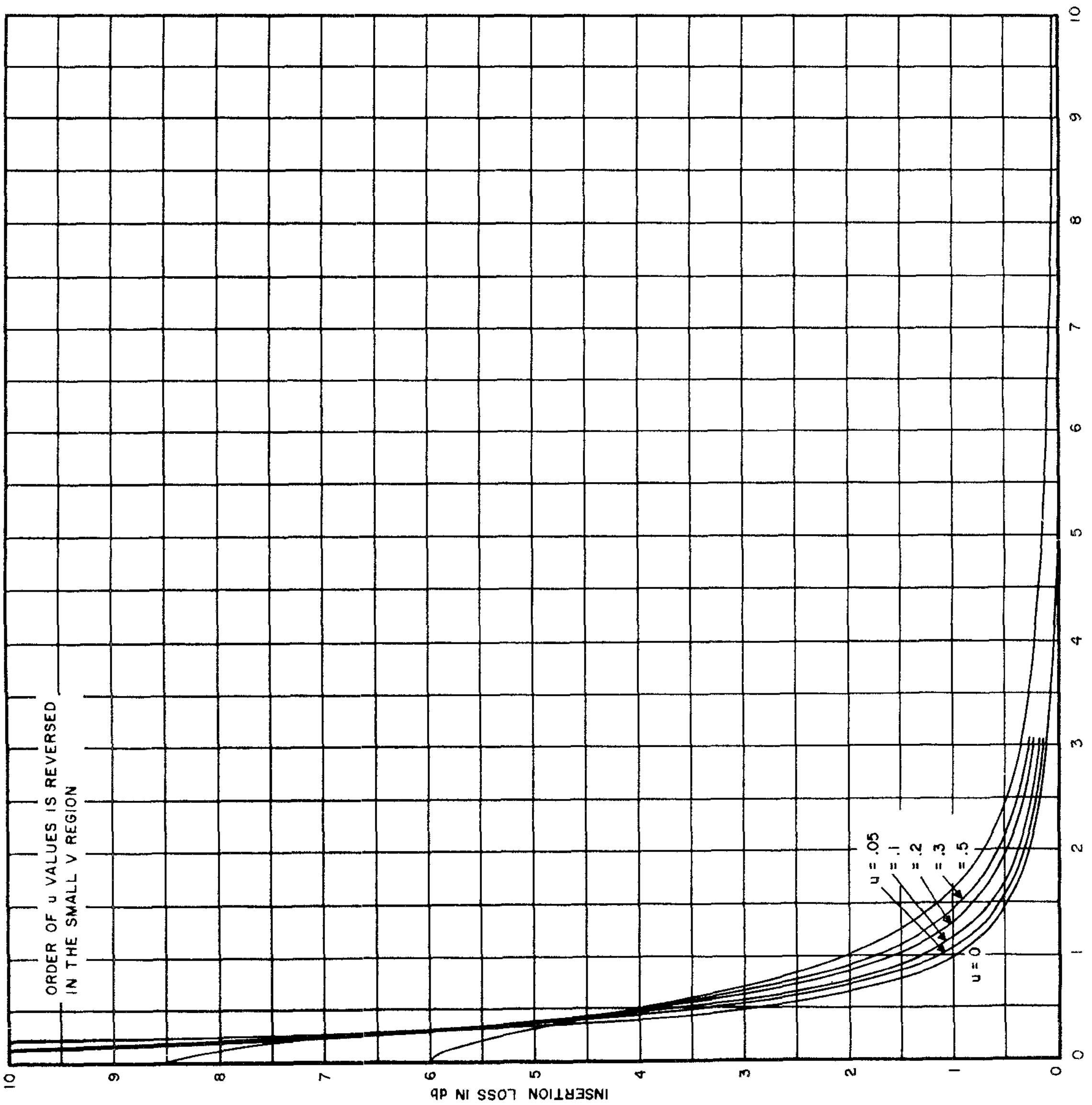

Fig. 4. Calculated pass-band insertion loss vs. normalized frequency with u as a parameter of dissipation ($n=1$ resonator).

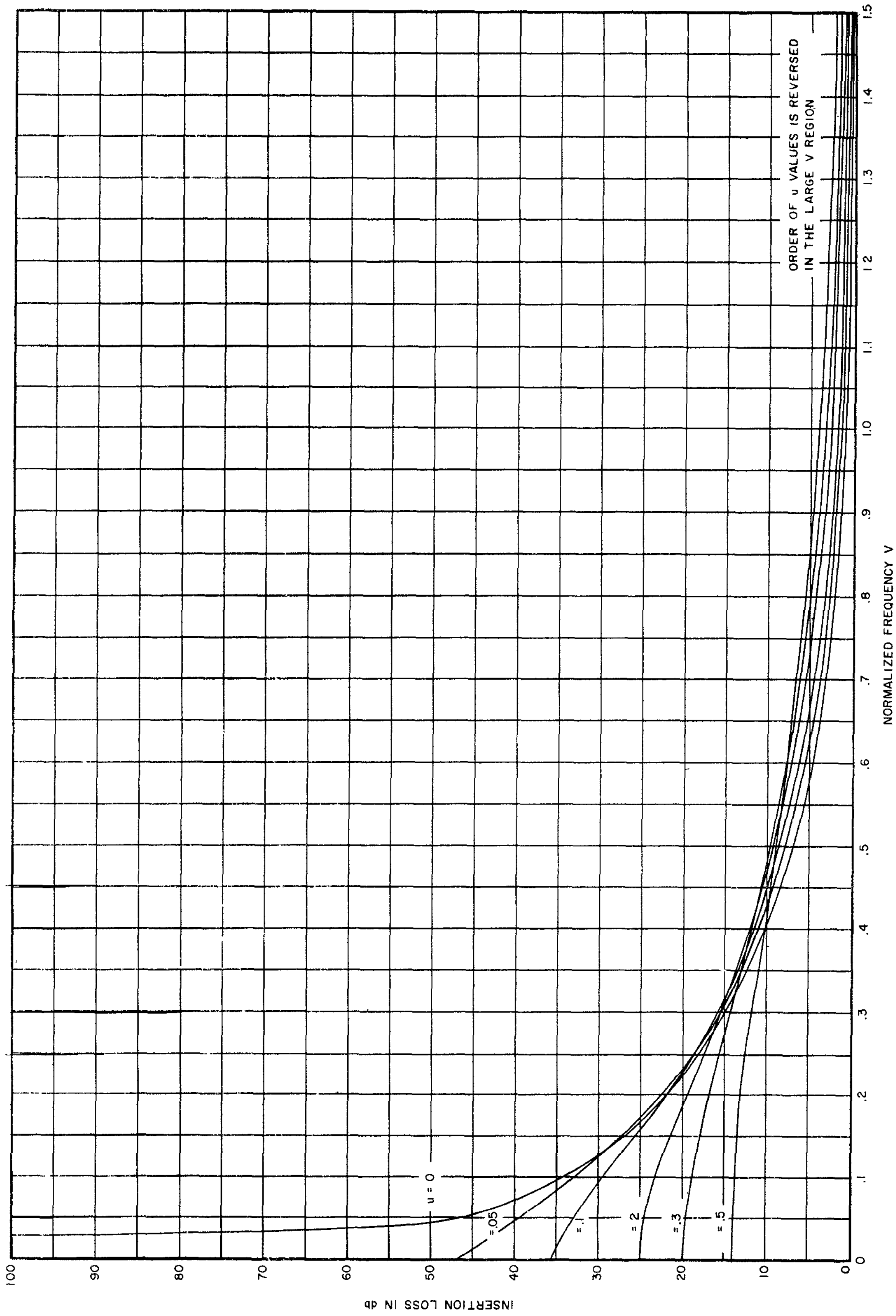

Fig. 5. Calculated stop-band insertion loss vs. normalized frequency with u as a parameter of dissipation ($n=2$ resonators).

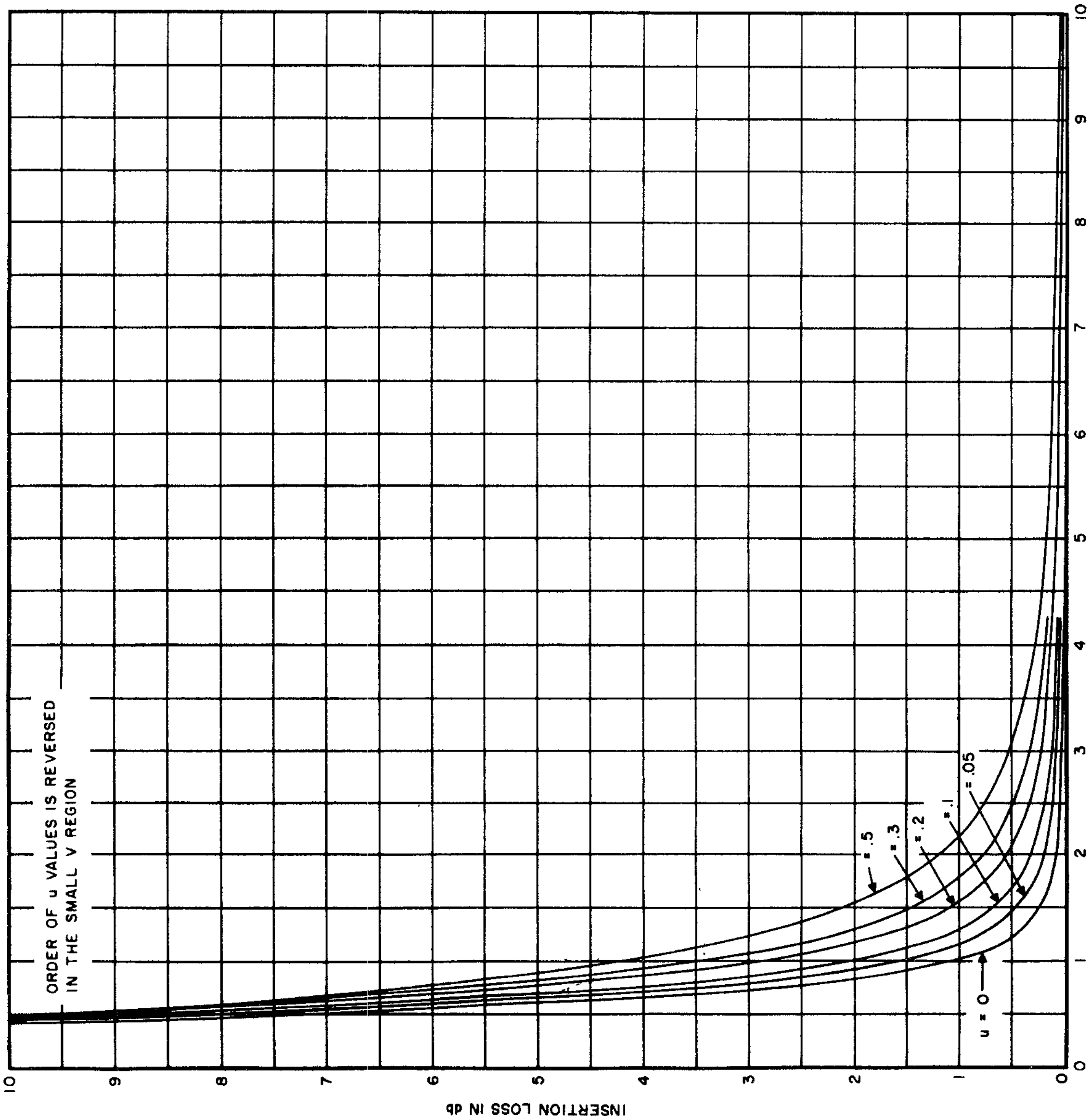

Fig. 6. Calculated pass-band insertion loss vs. normalized frequency with u as a parameter of dissipation ($n=2$ resonators).

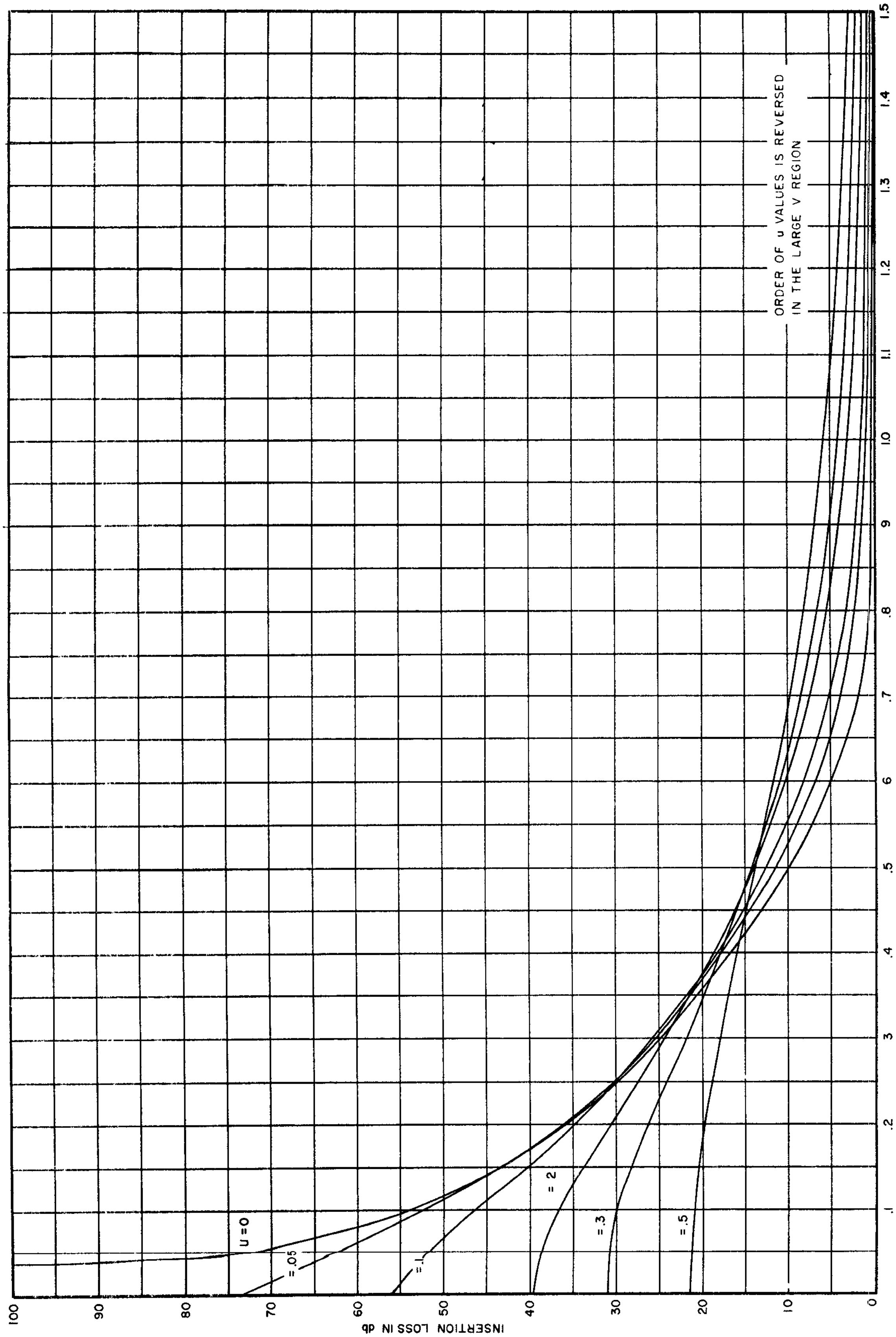

Fig. 7. Calculated stop-band insertion loss vs. normalized frequency with u as a parameter of dissipation ($n=3$ resonators).

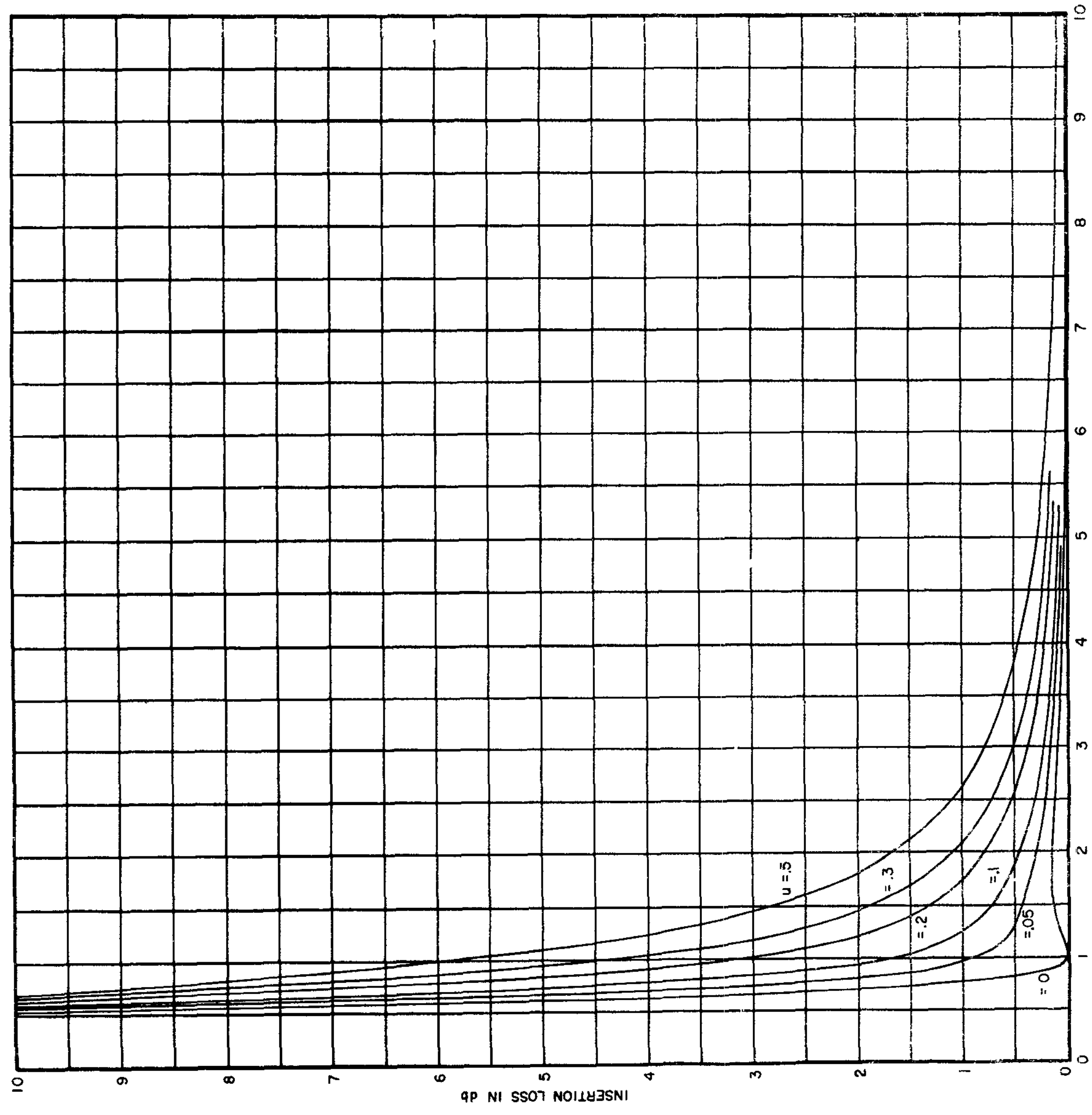

Fig. 8. Calculated pass-band insertion loss vs. normalized frequency with u as a parameter of dissipation ($n=3$ resonators).

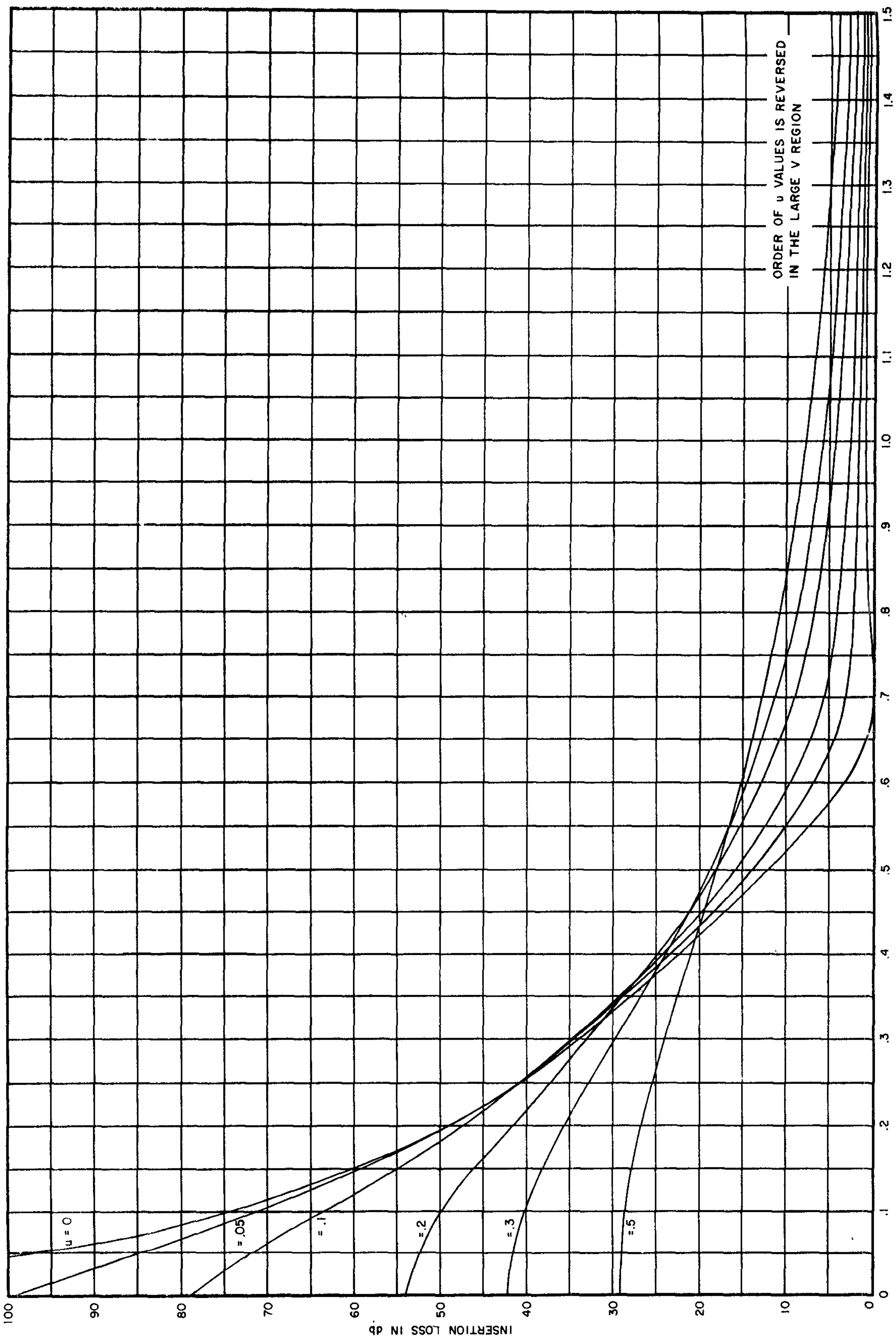

Fig. 9. Calculated stop-band insertion loss vs. normalized frequency with u as a parameter of dissipation ($n=4$ resonators).

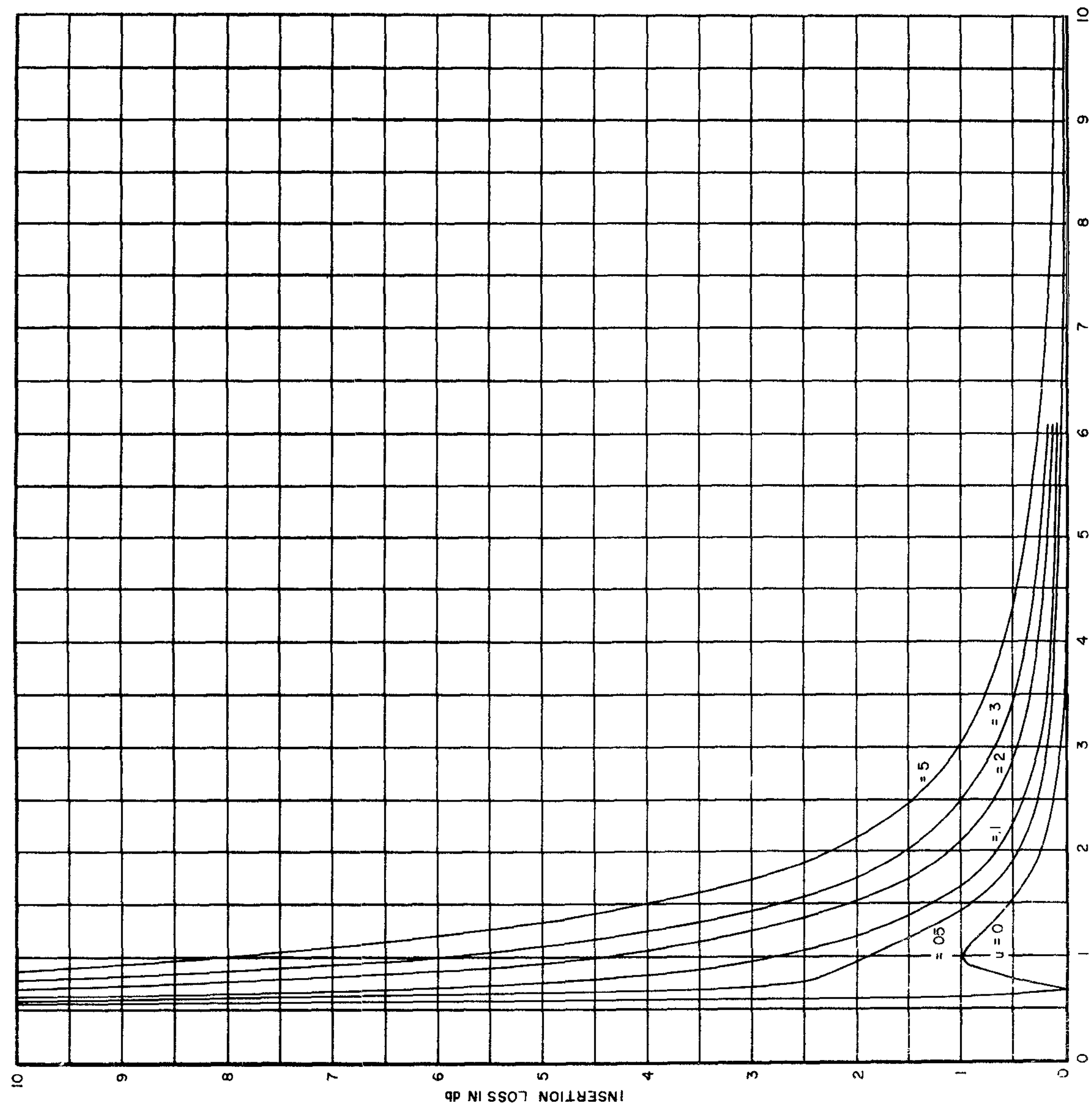

Fig. 10. Calculated pass-band insertion loss vs. normalized frequency with u as a parameter of dissipation ($n=4$ resonators).

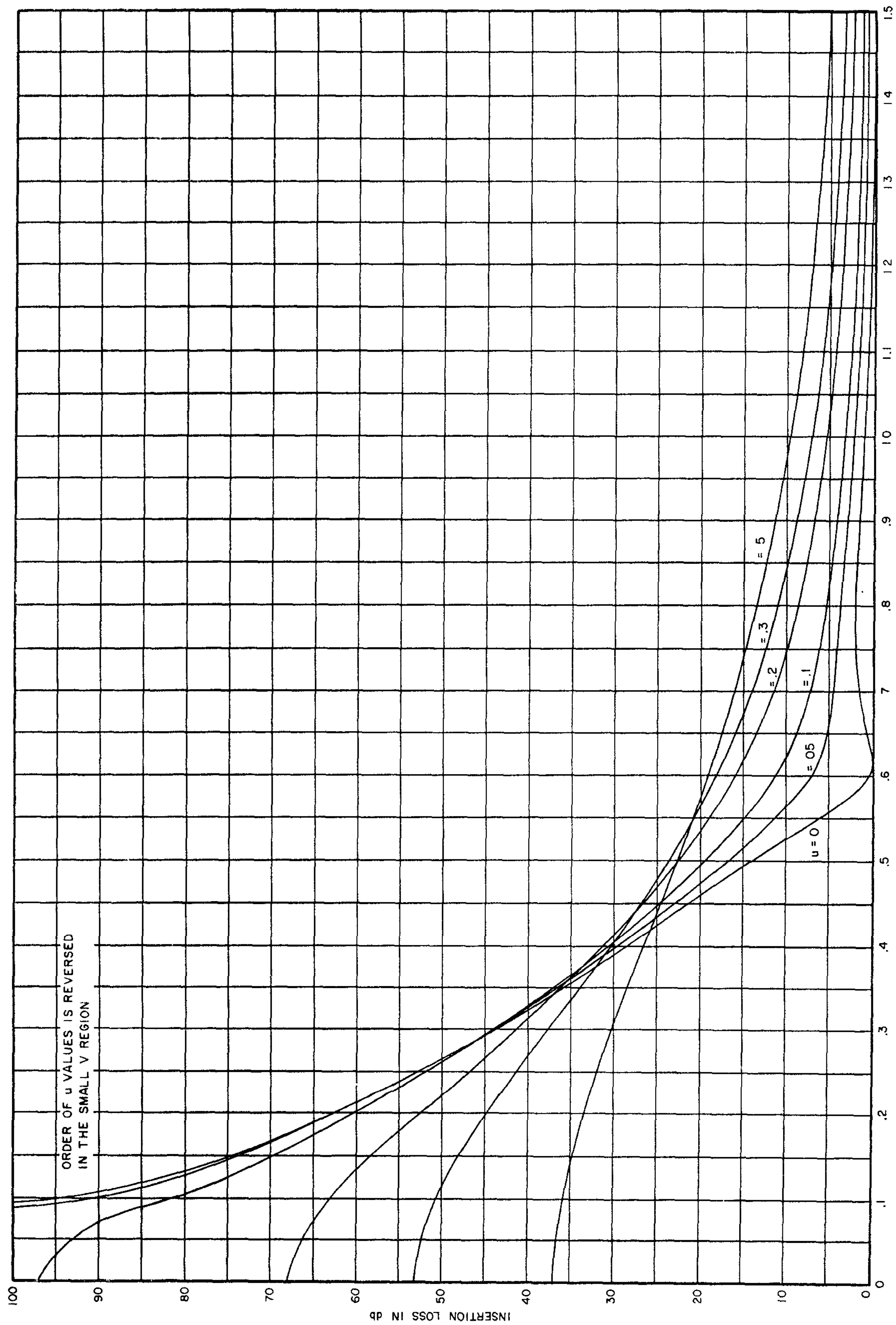

Fig. 11. Calculated stop-band insertion loss vs. normalized frequency with u as a parameter of dissipation ($n=5$ resonators).

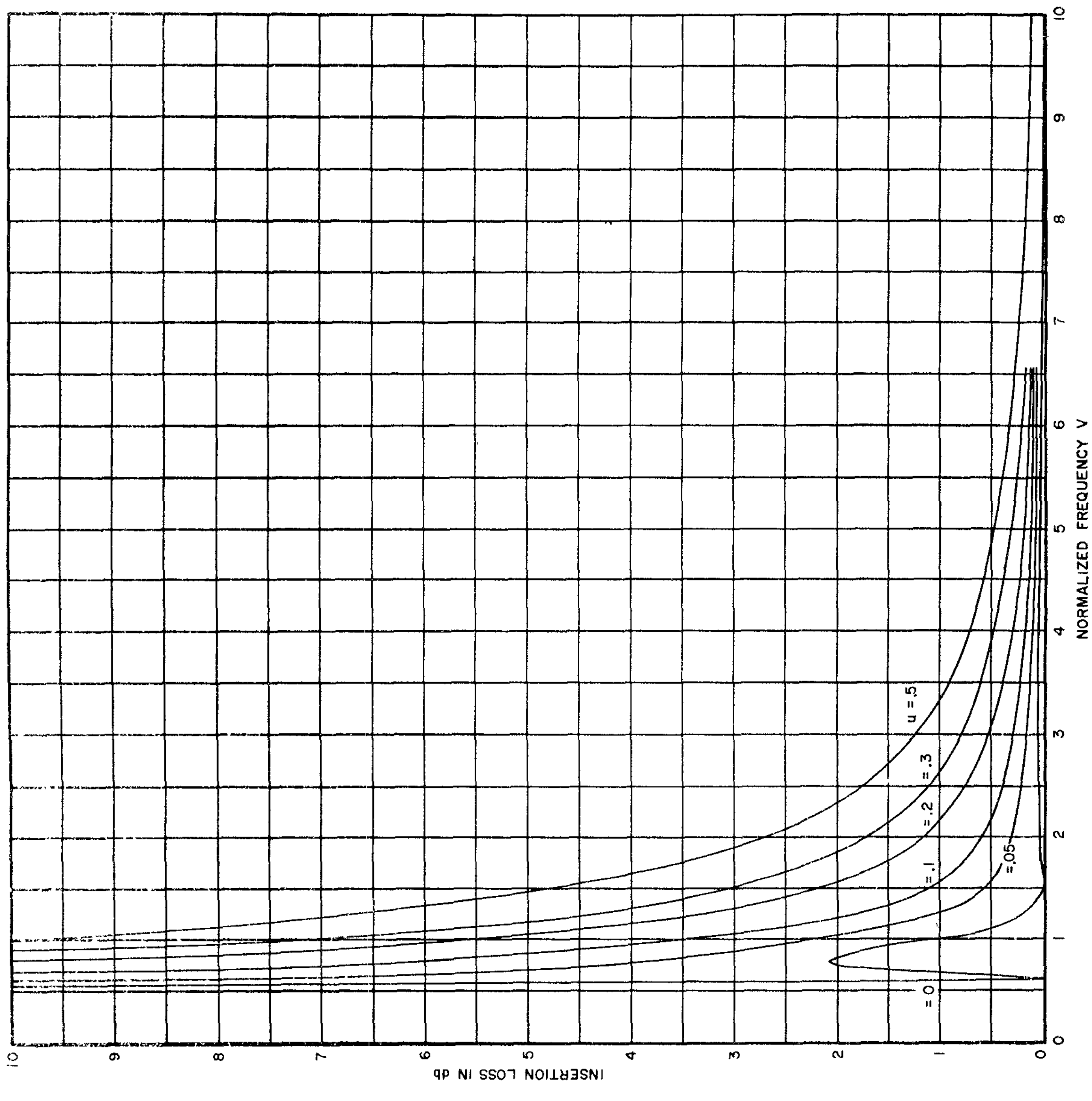

Fig. 12. Calculated pass-band insertion loss vs. normalized frequency with u as a parameter of dissipation ($n=5$ resonators).

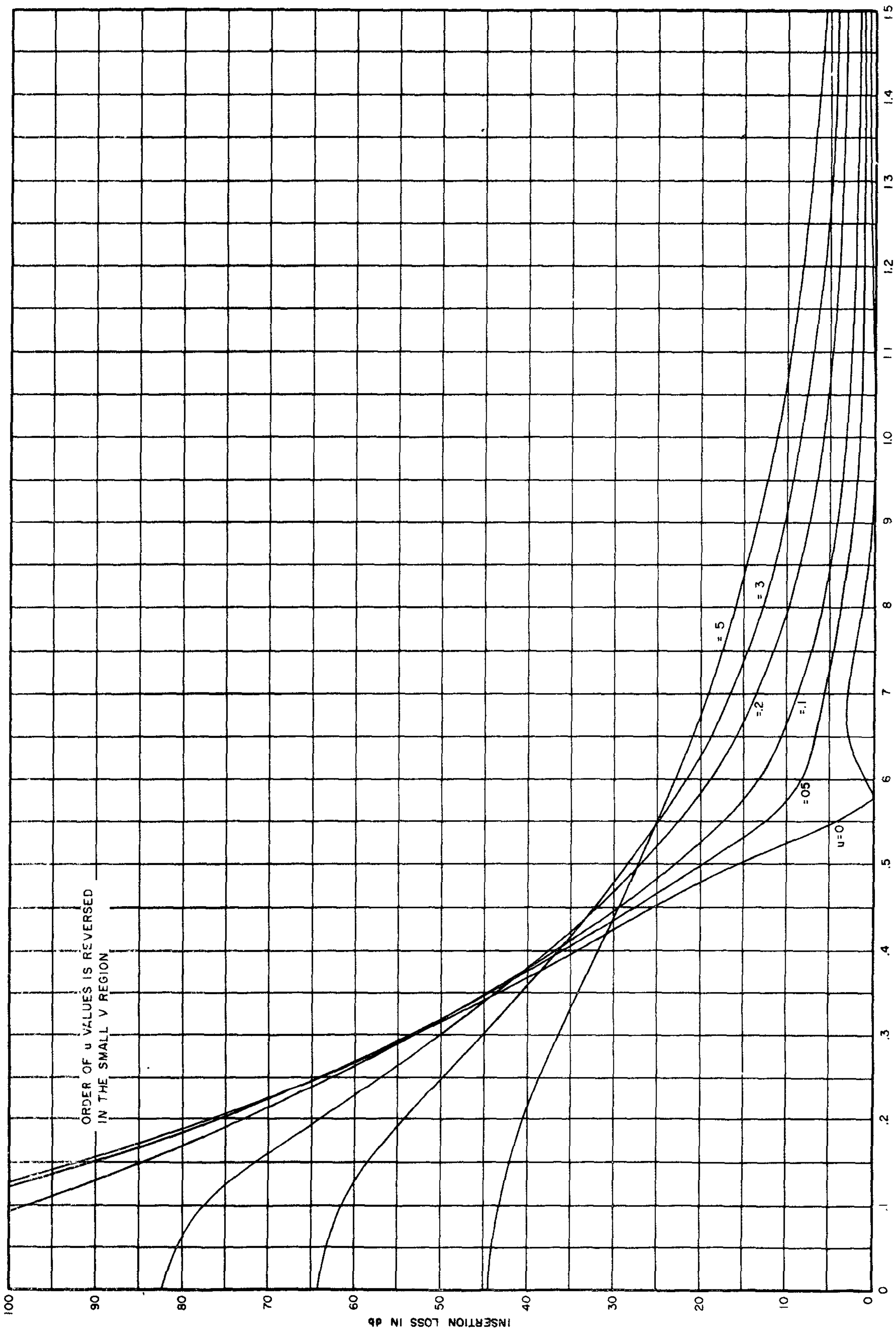

Fig. 13. Calculated stop-band insertion loss vs. normalized frequency with u as a parameter of dissipation ($n=6$ resonators).

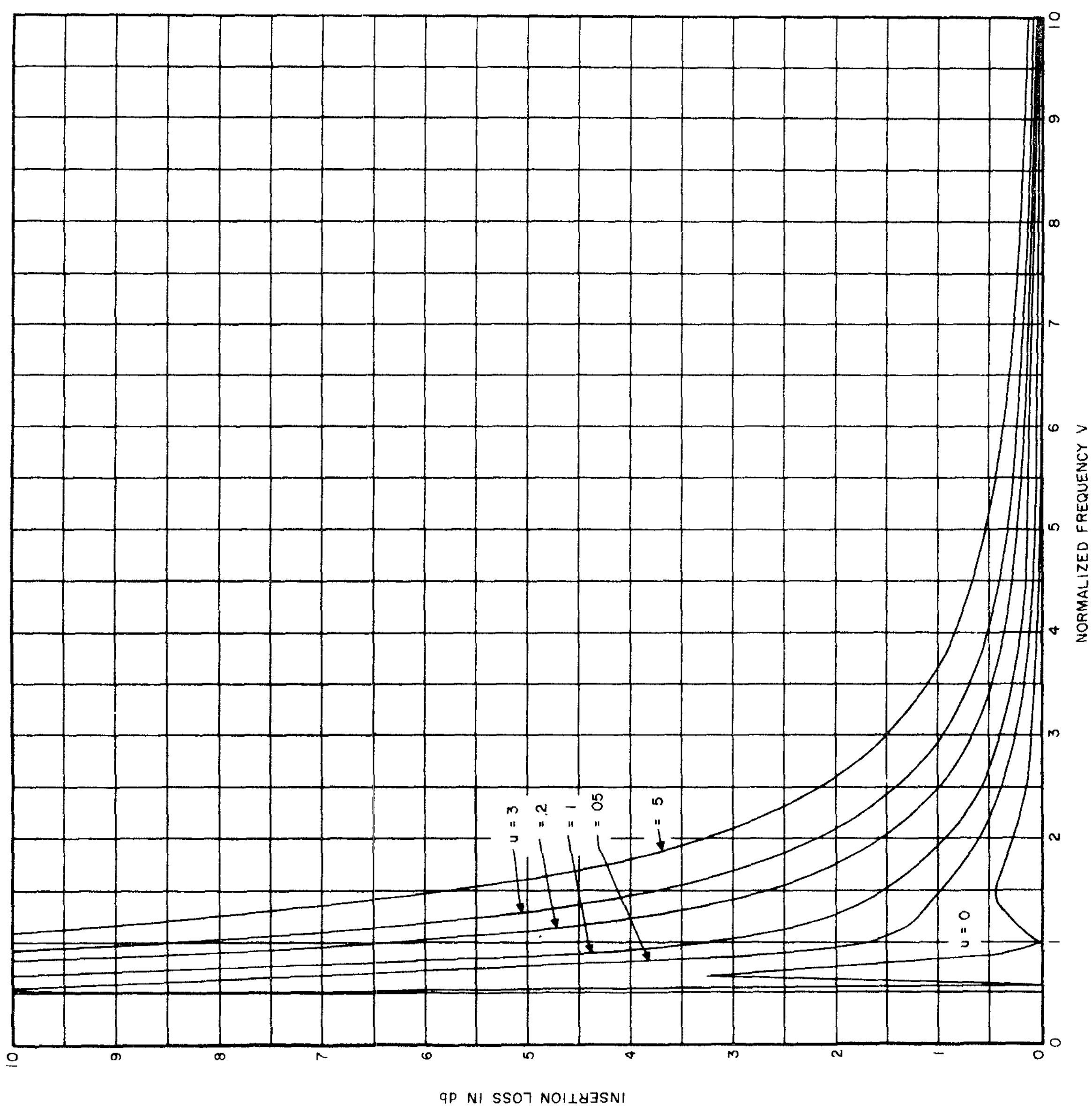

Fig. 14. Calculated pass-band insertion loss vs. normalized frequency with u as a parameter of dissipation ($n=6$ resonators)

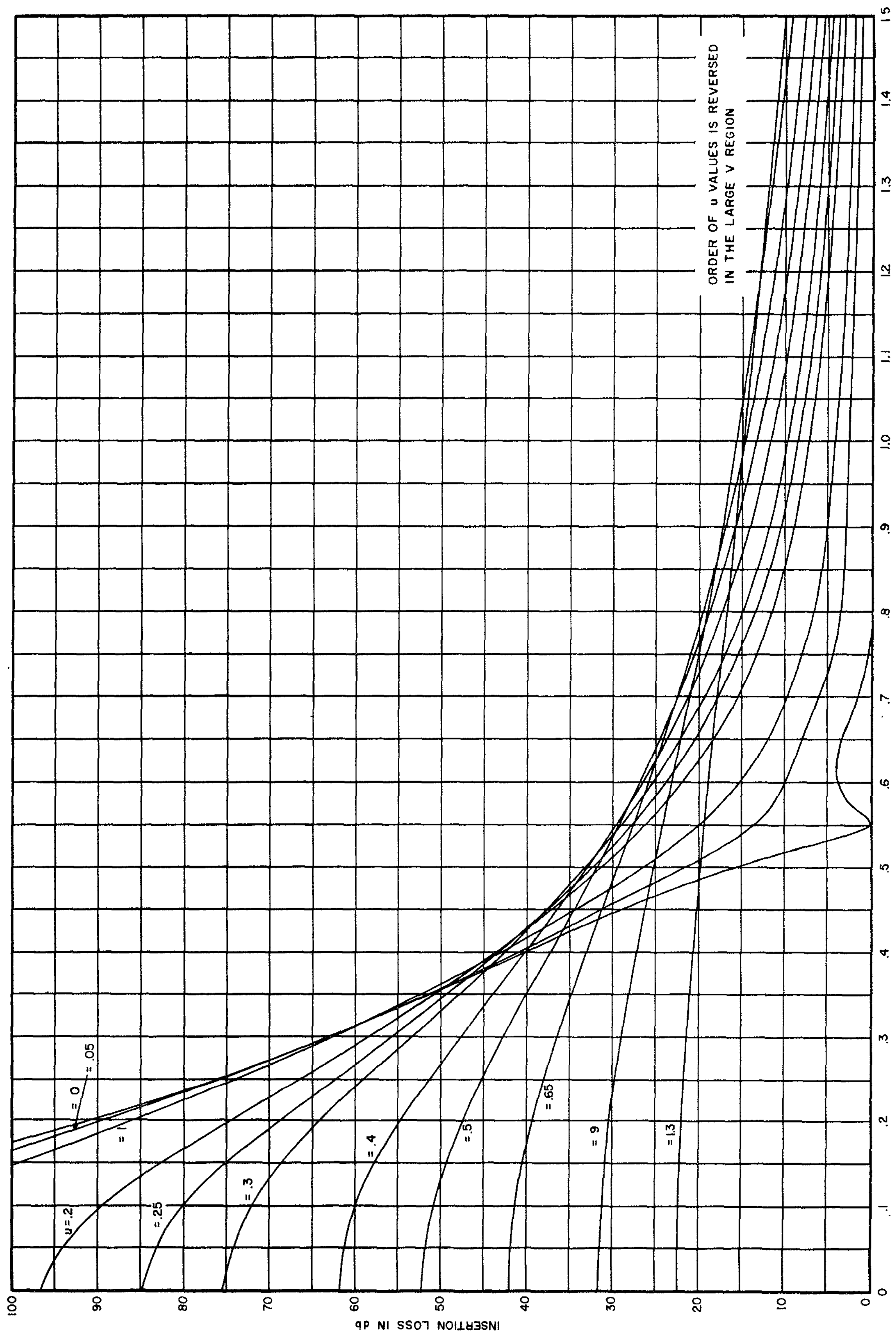

Fig. 15. Calculated stop-band insertion loss vs. normalized frequency with u as a parameter of dissipation ($n=7$ resonators).

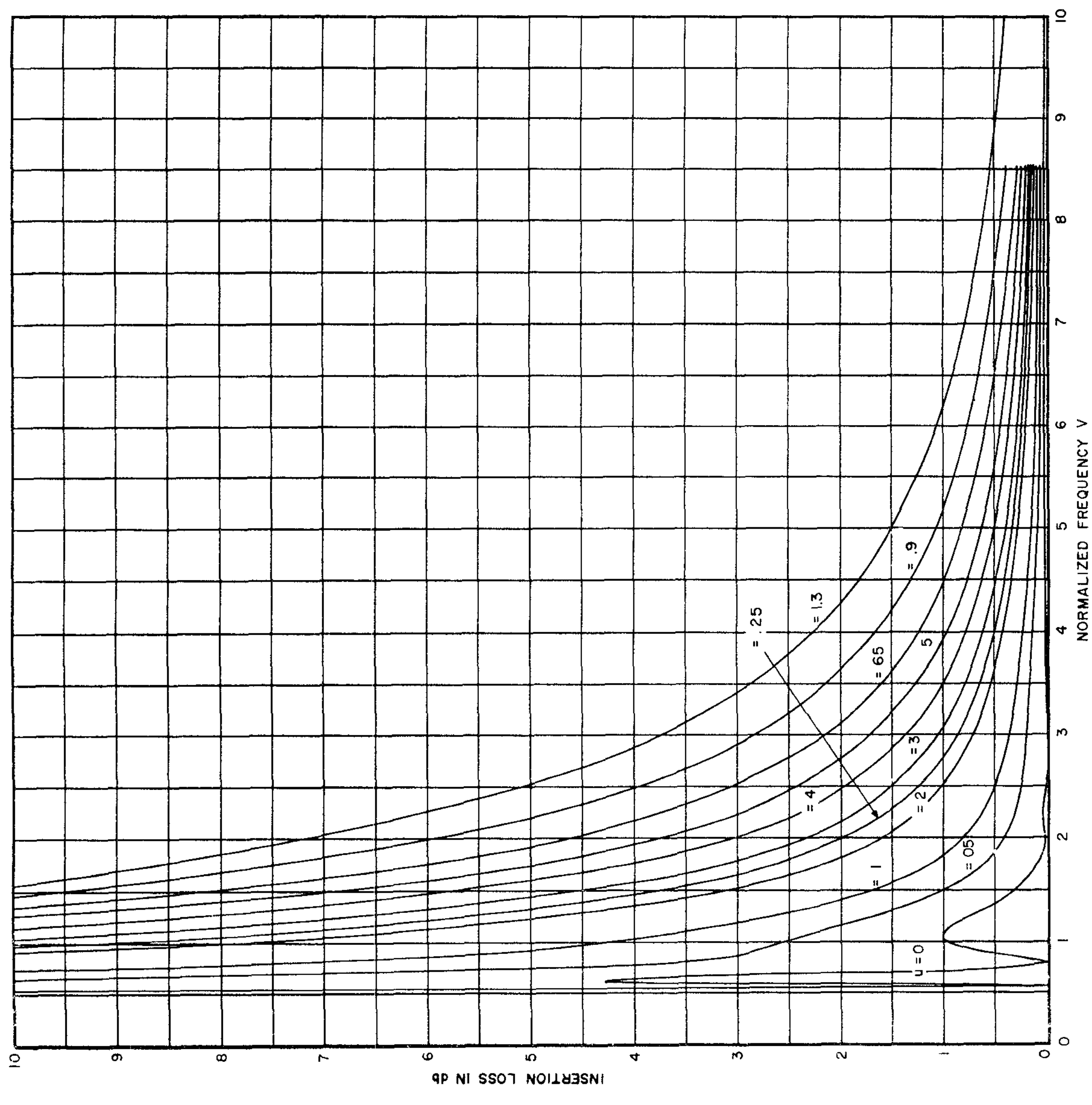

Fig. 16. Calculated pass-band insertion loss vs. normalized frequency with u as a parameter of dissipation ($n=7$ resonators).

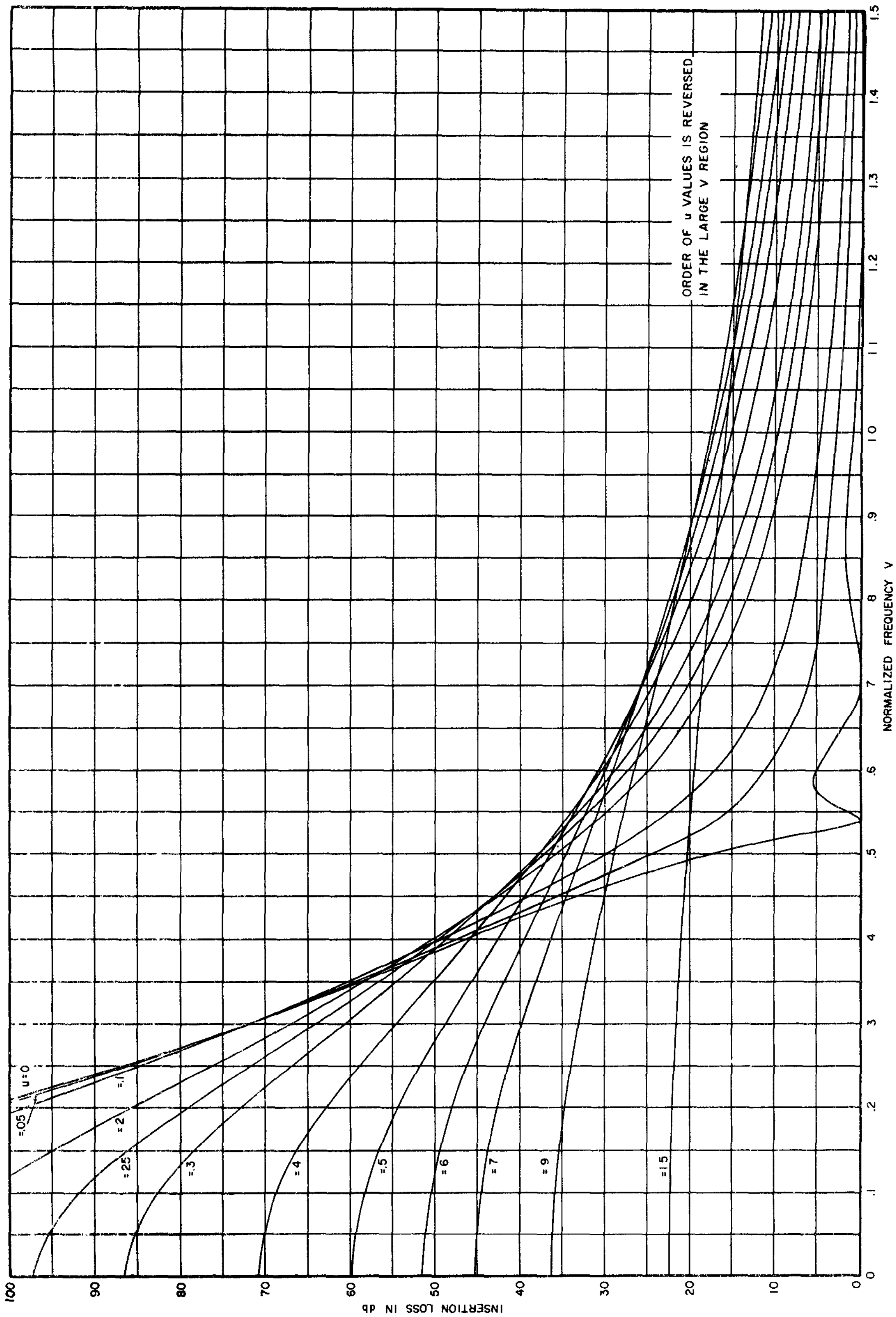

Fig. 17. Calculated stop-band insertion loss vs. normalized frequency with u as a parameter of dissipation ($n=8$ resonators).

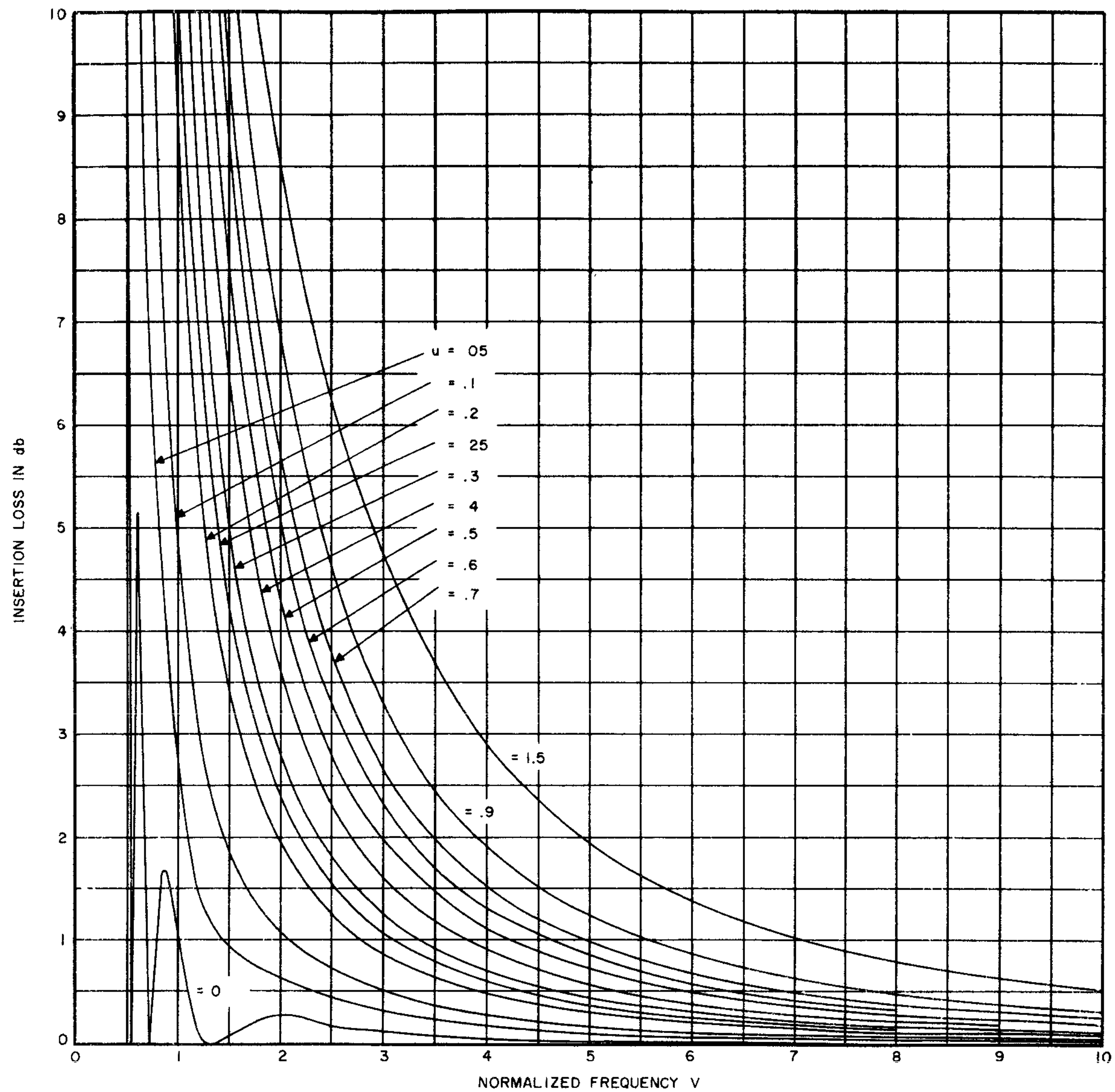

Fig. 18. Calculated pass-band insertion loss vs. normalized frequency with u as a parameter of dissipation ($n=8$ resonators).

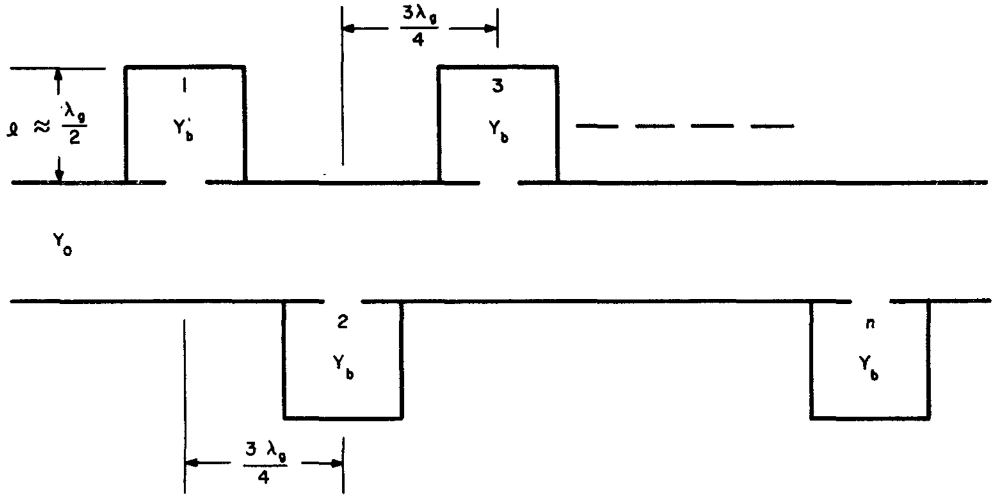

(a)

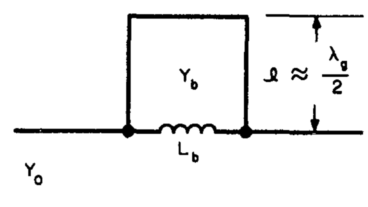

(b)

$$\omega_0 L_b = \frac{1}{Y_b \tan \phi_0}$$

$$\frac{\pi}{2} + \phi_0 = \frac{2\pi \ell}{\lambda_g}$$

$$G_{(\phi_0)} = \frac{2b}{Y_b} = \frac{2V_1}{WY_b}$$

$$Q_u = \frac{V_1}{uW}$$

NOTES:

1. $G_{(\phi_0)} \approx 2F_{(\phi_0)}$

   THIS APPROXIMATION HOLDS FOR MOST CASES. REFERENCE 1 SHOULD BE CONSULTED FOR A MORE EXACT DETERMINATION OF $G_{(\phi_0)}$.

   TABLES OF $F_{(\phi_0)}$ ARE GIVEN IN REFERENCE 1

2. u AND V_1 ARE DETERMINED FROM THE PROCEDURE GIVEN IN SECTION IV

(c)

Fig. 19. Summary of waveguide filter design. (a) Waveguide filter. (b) Typical resonator coupled to the main transmission line. (c) Design formulas.

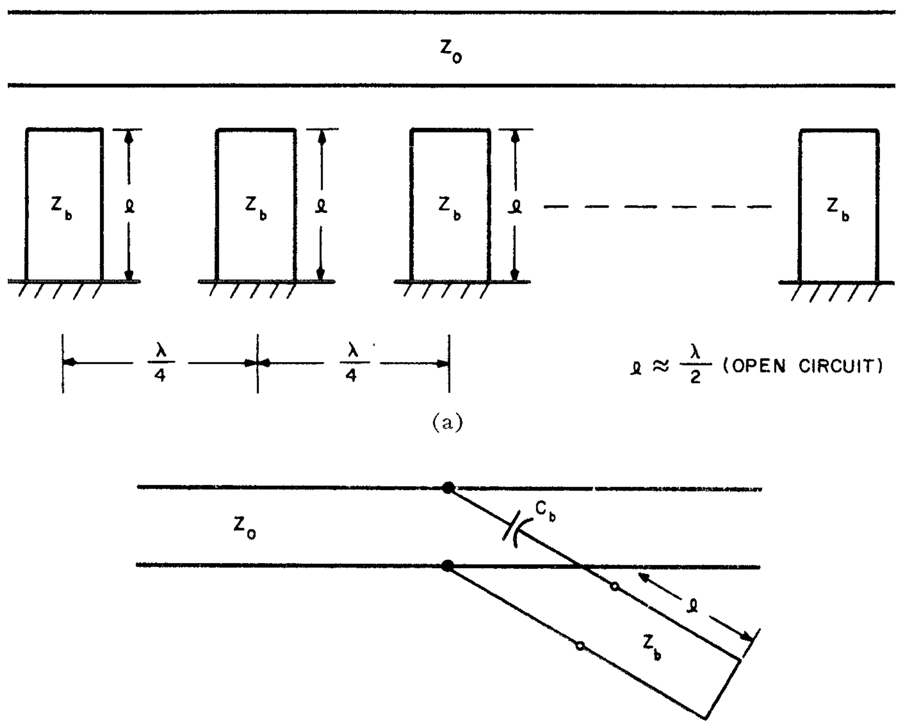

$$\omega_0 C_b = \frac{1}{Z_b \tan \phi_0}$$

$$\phi_0 = \frac{2\pi \ell}{\lambda}$$

$$F_{(\phi_0)} = \frac{2X}{Z_b} = \frac{2V_1}{WZ_b}$$

$$Q_u = \frac{V_1}{uW}$$

NOTES:

1. TABLES OF $F_{(\phi_0)}$ ARE GIVEN IN REFERENCE 1

2. u AND V_1 ARE DETERMINED FROM THE PROCEDURE GIVEN IN SECTION IV

(c)

Fig. 20. Summary of coaxial or strip-transmission-line filter design (λ/4 short-circuit resonators). (a) Coaxial or strip-transmission-line filter. (b) Typical resonator coupled to the main transmission line. (c) Design formulas.

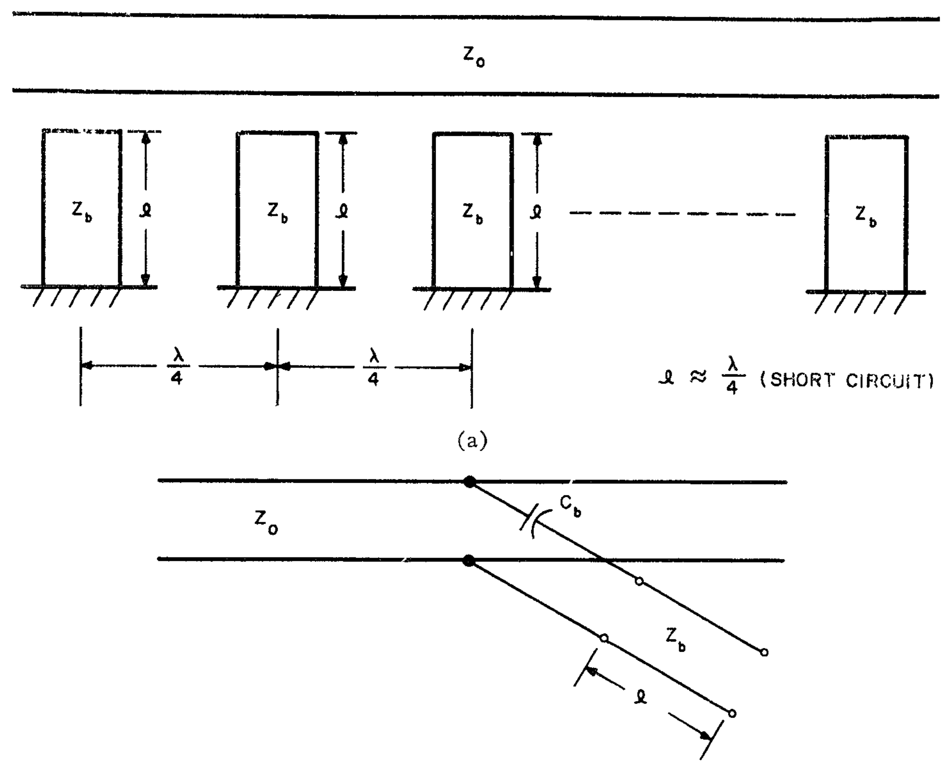

$$\omega_0 C_b = \frac{1}{Z_b \tan \phi_0}$$

$$\frac{\pi}{2} + \phi_0 = \frac{2\pi \ell}{\lambda}$$

$$G_{(\phi_0)} = \frac{2X}{Z_b} = \frac{2V_1}{WZ_b}$$

$$Q_u = \frac{V_1}{uW}$$

NOTES:

1. $G_{(\phi_0)} \approx 2F_{(\phi_0)}$

THIS APPROXIMATION HOLDS FOR MOST CASES. REFERENCE 1 SHOULD BE CONSULTED FOR A MORE EXACT DETERMINATION OF $G_{(\phi_0)}$. TABLES OF $F_{(\phi_0)}$ ARE GIVEN IN REFERENCE 1.

2. u AND V_1 ARE DETERMINED FROM THE PROCEDURE GIVEN IN SECTION IV

(c)

Fig. 21. Summary of coaxial or strip-transmission-line filters (λ/2 open-circuit resonators). (a) Coaxial or strip-transmission-line filter. (b) Typical resonator coupled to the main transmission line. (c) Design formulas.

III. Useful Relationships

Certain properties of equal-element filters, which are derived in this section, are important to consider when applying the design procedure described in Section IV.

Stop- and Pass-Band Loss

The insertion loss in the high-rejection region ($v \ll 1$ and $u \ll v$) can be approximated by noting that M_n of (37) becomes

$$M_n \approx \frac{1}{X^n} = \frac{1}{(jv)^n} \tag{8}$$

or

$$L \approx 10 \log \frac{1}{4v^{2n}} \cdot \tag{9}$$

In the low-loss region ($v \gg 1$ and $u \ll v$), we can solve for the dissipation loss (the difference between the total insertion loss with $u \neq 0$ and with $u = 0$) by noting that

$$M_n \approx 2 + \frac{n}{u - jv} \tag{10}$$

$$|M_n|^2 \approx 4 + \frac{4nu}{v^2} \tag{11}$$

$$L = 10 \log \frac{|M_n|^2}{4} \approx 10 \log \left(1 + \frac{nu}{v^2}\right)$$

$$\approx 4.34 \frac{nu}{v^2} \text{ dB}. \tag{12}$$

This formula for small dissipation loss is in agreement with the relationship given in Fig. 8 of reference [1], for the case where all g values are equal.

Element Values for Minimum Pass-Band Loss

The following shows that the equal-element filter yields the minimum pass-band dissipation loss for a specified rejection loss and rejection bandwidth. Assumed are small dissipation (less than 0.2 dB per resonator in the pass band), equal values of Q_u for all resonators, high rejection (at least 10 dB per resonator), and $g_0 = g_{n+1} = 1$.

For high rejection near the band center, the insertion loss of a band-stop filter having low-pass prototype element values $g_1, g_2 \cdots g_n$ is given by (5) and (6) of reference [3]:

$$L = 20 \log (\omega')^n g_1 g_2 \cdots g_n - 6 \text{ dB} \tag{13}$$

where $\omega' \gg 1$.

The dissipation loss in the pass band (for small dissipation) is obtained from Fig. 8 of reference [1]:

$$L = \frac{1.086 w \omega_1'}{Q_u} \left(\frac{\omega}{\omega - \omega_0}\right)^2 (g_1 + g_2 + \cdots g_n) \text{ dB}. \tag{14}$$

For a fixed rejection at a specified $\omega' = \omega_s' = \alpha\omega_1'$ (where α is a specified constant), we have

$$(\omega_s')^n g_1 g_2 \cdots g_n = \text{constant}$$

or

$$(\omega_1')^n g_1 g_2 \cdots g_n = \text{constant} \tag{15}$$

and at a fixed $\omega - \omega_0$, Q_u, and w, we desire

$$\omega_1'(g_1 + g_2 + \cdots g_n) = \text{minimum}. \tag{16}$$

The derivatives of both expressions must therefore be zero, that is,

$$\frac{\delta(\omega_1' g_1)}{\omega_1' g_1} + \frac{\delta(\omega_1' g_2)}{\omega_1' g_2} + \cdots \frac{\delta(\omega_1' g_n)}{\omega_1' g_n} = 0$$

$$\delta(\omega_1' g_1) + \delta(\omega_1' g_2) + \cdots \delta(\omega_1' g_n) = 0. \tag{17}$$

These equations can be satisfied only when $g_1 = g_2 = \cdots g_n$. An equal-element design will therefore yield the lowest pass-band dissipation loss for a fixed rejection characteristic. Although small dissipation was assumed, the equal-element filter is a very good choice for larger pass-band dissipation (at least 1 dB per resonator).

Optimum Number of Resonators

For a specified rejection bandwidth, the loss in the pass band (at a specified frequency from that of maximum rejection) will be a function of the number of resonators used and their unloaded Q's. For a given value of unloaded Q and the correct number of resonators, the minimum loss in the pass band can be calculated. Formulas for the optimum number of resonators and the resultant minimum insertion loss are presented in the following paragraphs.

Using (9) and assuming a minimum stop-band loss (L_s) at a normalized frequency deviation $v = v_s$ gives

$$L_s = 20\, n \log \frac{1}{v_s} - 6 \text{ dB}. \tag{18}$$

The loss at a pass frequency v_1 is defined from (12) as

$$L_1 = \frac{4.34nu}{v_1^2} = \frac{4.34nu}{\alpha^2 v_s^2} \text{ dB} \tag{19}$$

where α is defined as the ratio of the pass bandwidth to the stop bandwidth (v_1/v_s). By noting that

$$n = \frac{L_s + 6}{20 \log 1/v_s} \tag{20}$$

$$u = \frac{v_s}{w_s Q_u} \tag{21}$$

where w_s is the fractional stop bandwidth, L_p can be expressed as

$$L_p = \frac{4.34(L_s + 6)}{20 w_s Q_u \alpha v_s \log 1/v_s} \text{ dB}. \tag{22}$$

Differentiating L_p with respect to v_s and setting it equal to zero gives $\log 1/v_s = 0.434$, or

$$n = \frac{L_s + 6}{8.68} \cdot \tag{23}$$

This is similar to the optimum n for the band-pass case [4], [5].

Using this n gives an $L_{p_{\min}}$ of

$$L_{p_{\min}} = \frac{27.2(L_s + 6)}{20 w_s Q_u \alpha} \cdot \tag{24}$$

IV. Design Procedure

General

The usual band-stop filter design requires a minimum rejection within a specified frequency band and a maximum pass-band loss beyond a specified band. The first problem is to choose the correct n (number of resonant circuits). Examination of the response curves (Figs. 3 through 18) shows that more than one value of n will often satisfy the requirements. The choice is often simplified by the fact that an optimum n exists for a specified rejection, as shown in the previous section. (The selection of n is further discussed in the following paragraph.) For the moment, let us assume that n has been selected.

It is now necessary to determine u and v_1. If the loss is small ($u<0.1$), approximate formulas (9) and (12) do not require the use of the response curves; these formulas are applied in this section. For larger losses, the response curves are needed. With the aid of a successive approximation procedure, values of u and v_1 can be obtained. Finally, the coupling reactance and resonator length values can be determined from the knowledge of u and v_1.

Number of Resonators

Given a minimum stop-band loss L_s with a bandwidth B_s, and a pass-band loss L_1 with a bandwidth B_1, the number of resonators can be determined by means of (23).

Other choices of n are possible, but they will require resonators with higher values of Q_u to achieve the desired response.

Determination of u and v

Having chosen n, the next step is to assume $u=0$ (lossless case) and solve for a trial value of v_s (the v corresponding to the desired rejection) using (18). This gives

$$v_s = \frac{1}{\log^{-1}\left(\frac{L_s + 6}{20n}\right)} \tag{25}$$

where L_s is expressed in dB.

A trial value of u is then obtained from (19) and is

$$u = \frac{\alpha^2 v_s^2 L_1}{4.34n} \tag{26}$$

where L_1 is expressed in dB, and $\alpha = v_1/v_s$. Using this value of u, a new v_s is determined from the appropriate insertion-loss curve. This can again be used to compute a more accurate u value using (27). If the new u has changed significantly (more than 10 percent) from the trial value, another v_s must be determined. This process can be repeated until an exact u is determined to match both the stop- and the pass-band requirements simultaneously. In most cases, the procedure need not be repeated more than once after the trial value has been obtained. The knowledge of u enables us to obtain an exact v_s which, in turn, yields $v_1 = \alpha v_s$, the desired information for computing the coupling reactances and resonator lengths by means of the formulas given in Figs. 19, 20, and 21.

V. Design Examples and Experimental Verification

The design procedures for waveguide and coaxial-line band-stop filters are presented in this section, together with measured data. In addition to showing close agreement between measured and calculated responses, the new dissipative design is clearly shown to be superior to the previous lossless design.

Example 1

Required: A WR 159 waveguide filter having the following characteristics:

Center frequency	6000 Mc
Insertion loss in the stop band	43 dB over a ± 1.25-Mc bandwidth
Insertion loss in the pass band	0.25 dB maximum at ± 13.5 Mc away from the center frequency ($\alpha = 10.8$).

The parameters that must be determined are number of resonators, required unloaded Q's, coupling reactances, and resonator lengths.

The number of resonators is selected using (23). For $L_s = 43$ dB, the calculated value of $n = 5.64$; the selection of n therefore appears to either five or six resonators. The $n=6$ case is considered here. Using Fig. 13, a trial $v_s = 0.35$ is obtained for $u=0$. Using Fig. 14, a trial value of $u=0.10$ is obtained for $v_1 = \alpha v_s = 3.78$ and $L_p = 0.25$ dB. Using this u in Fig. 13 gives $v_s = 0.36$. This value of v_s is sufficiently close to the first trial value so that the procedure does not have to be continued and the values $u=0.10$ and $v_s = 0.36$ can be used in the design.

The required unloaded resonator Q is determined from (21):

$$Q_u = \frac{v_s}{w_s u} = \frac{0.36}{\frac{2.5}{6000}\left(\frac{\lambda_g}{\lambda}\right)^2 \times 0.1} = 5330$$

where $(\lambda_g/\lambda)^2 = 1.62$ at 6000 Mc in WR 159 waveguide.

A similar procedure for $n=5$ gives $v_s=0.31$ and $u=0.10$, resulting in $Q_u=4600$.

These results indicate a choice of $n=5$. A four-resonator filter is also possible, but it would require a higher Q_u than either of the other two cases.

The filter will be designed using the model of Fig. 19 with $Y_b=Y_0$. The design requires knowledge of the susceptance slope parameter b/Y_0. For an equal-element filter, all b/Y_0 values are the same. The value of b/Y_0 from (7) and Fig. 2(b) is

$$\frac{b}{Y_0}=\frac{v_s}{w_s}=\frac{0.31}{\frac{2.5}{6000}\times 1.62}=459.$$

To obtain the resonator length, we note in Fig. 19 that

$$G_{(\phi_0)}=2b/Y_b=2b/Y_0=918$$
$$F_{(\phi_0)}\approx \tfrac{1}{2}G_{(\phi_0)}=459.$$

The value of ϕ_0, obtained from Table II of reference [1], is 86.64 degrees. This means that each resonator is 176.64 degrees in electrical length, or

$$l=\frac{176.64}{180}\frac{\lambda_g}{2}=1.222 \text{ inches}$$

and the normalized coupling susceptance

$$\frac{B_b}{Y_b}=\frac{B_b}{Y_0}=\tan\theta_0=17.04.$$

The dimensions of the coupling apertures are determined by solving for the magnetic polarizability M' using Bethe's theory [6]–[8]. The expression is

$$\frac{B_b}{Y_0}=\frac{\lambda_g ab'}{4\pi M'} \tag{27}$$

where a and b' are the waveguide dimensions 1.590 and 0.795 inches.

Using reference [1], the 0.0147 value of M' is converted into the dimensions for a rectangular aperture with length = 0.450 inch and width = 0.196 inch. These values are used for the first trial. The actual dimensions required for the coupling susceptance in each of the five resonators are set by taking measurements on a single-resonator filter. For $n=1$ and $u=0.10$, we obtain (from Fig. 4) a value of $v_1=0.58$ for 3 dB of insertion loss. Substituting $b/Y_0=459$ and $(\lambda_g/\lambda)^2=1.62$ in (28) gives the 3-dB bandwidth of 4.69 Mc for $f_0=6000$ Mc:

$$w=\frac{\Delta f}{f_0}\left(\frac{\lambda_g}{\lambda}\right)^2=\frac{v_1}{b/Y_0}. \tag{28}$$

The actual aperture dimensions required for a 4.69-Mc, 3-dB bandwidth in a single-resonator filter were length = 0.450 inch and width = 0.221 inch. The aperture thickness was 0.020 inch.

Figure 22 shows the close agreement between the theoretical curve and the measured values for the five-section band-reject filter. Another interesting comparison is between the dissipative band-stop filter design outlined here and the design outlined in reference [1]. The pass-band loss at ±13.5 Mc for the dissipative design, both measured and calculated, and the loss calculated from the design in reference [1] are as follows:

Reference [1] design	0.77 dB
Dissipative design (calculated)	0.25 dB
Dissipative design (measured)	0.30 dB.

The dissipative design provides lower pass-band loss and closer control of the entire response.

Example 2

Required: A coaxial transmission-line filter of the type shown in Fig. 21, having the following characteristics:

Center frequency	291 Mc
Insertion loss in the stop band	50 dB over ±3 Mc
Number of resonators	5.

Requirements for minimum pass-band loss and minimum size indicated the use of a 0.141-inch-diameter, 50-ohm, semirigid (Teflon-filled) coaxial line with an unloaded Q of 200 at 291 Mc.

The response curves of Fig. 11 show that 50 dB rejection occurs at $v_s=0.27$ for any u between 0 and 0.1. The actual value of u calculated from (21) is

$$u=\frac{v_s}{w_sQ_u}=\frac{0.27}{\frac{6}{291}\times 200}=0.065.$$

Only the coupling capacitance and the length of each resonator must be determined to complete the filter design.

With each resonator nominally one-half wavelength,

$$G_{(\phi_0)}=\frac{2x}{Z_0}=\frac{2v_s}{w_s}=\frac{2\times 0.27}{6/291}=26.2$$
$$F_{(\phi_0)}\approx \tfrac{1}{2}G_{(\phi_0)}=13.1$$

The value of ϕ_0 obtained from Table II of reference [1] is 70 degrees. The calculated resonator length is 12.75 inches. The coupling capacitance calculated from the expression

$$Z_0\tan\phi_0=\frac{1}{\omega_0 C_e}$$

is 3.98 pF. By adjusting for the desired single-resonator response, the optimum lumped capacitance was found to be 3.6 pF and the correct resonator length was 12.5 inches.

Figure 23 shows the close agreement between the measured and the calculated responses for insertion losses up to at least 50 dB. Although not shown, the pass-band response closely followed the theoretical curve for insertion losses as low as 0.1 dB. Here again, it is seen that the entire response can be accurately predicted and obtained in the presence of dissipation.

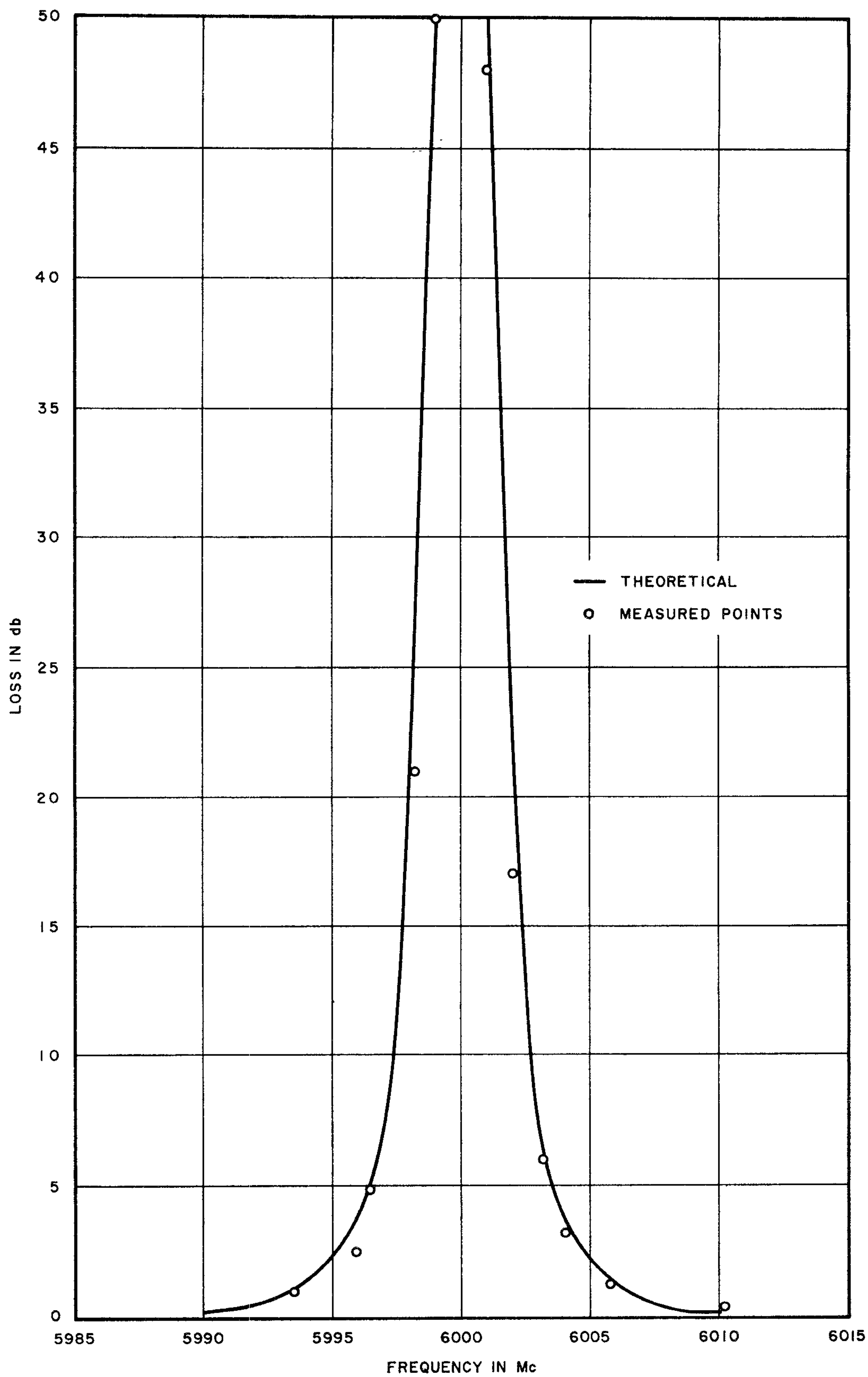

Fig. 22. Band-reject filter $n=5$.

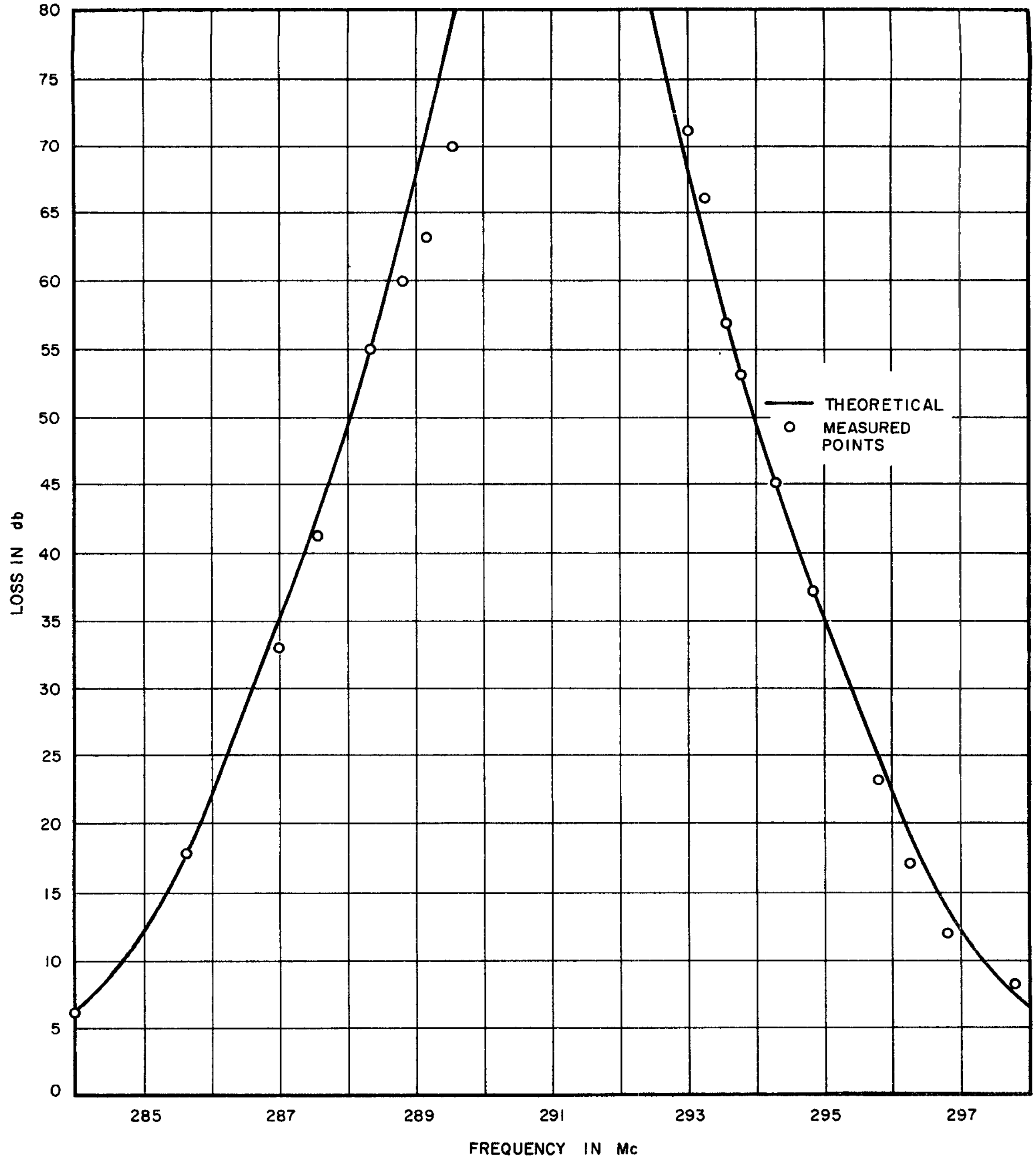

Fig. 23. UHF coaxial transmission-line band-reject filter $n=5$.

VI. Conclusions

The design procedures and experimental results presented show that dissipation effects in equal-element band-stop filters can be treated in an exact manner. The use of an equal-element filter is desired because it can yield a lower pass-band insertion loss for a specified rejection bandwidth than other designs and is simpler to construct. Another significant feature of the equal-element filter design is its ability to predict the entire response accurately, even in the presence of dissipation.

Appendix

Insertion Loss of an n-Resonator Equal-Element Band-Stop Filter

The insertion loss is obtained by multiplying the $ABCD$ matrix of the first element with each succeeding element. After an n-fold matrix multiplication, the overall $ABCD$ matrix is obtained. The insertion loss is then obtained from

$$L = 10 \log \frac{| A_\tau + B_\tau + C_\tau + D_\tau |^2}{4} \tag{29}$$

where we assume $g_{n+1}=g_0=1$.

Referring to Fig. 1(b), the matrix of the first shunt element is

$$\begin{pmatrix}1 & 0\\ Y & 1\end{pmatrix} = \begin{bmatrix}1 & 0\\ \dfrac{1}{\dfrac{1}{G_1}+\dfrac{1}{j\omega' g_1}} & 1\end{bmatrix}. \tag{30}$$

The matrix of the first series element is

$$\begin{pmatrix}1 & Z\\ 1 & 0\end{pmatrix} = \begin{bmatrix}1 & \dfrac{1}{\dfrac{1}{R_2}+\dfrac{1}{j\omega' g_2}}\\ 0 & 1\end{bmatrix}. \tag{31}$$

Since $g_1=g_2 \cdots =g_n$ and all Q_u's are equal, all R values are equal to all G values. We can therefore, with the aid of (2), define a normalized dissipation factor u, where

$$u = \frac{1}{R} = \frac{1}{G} = \frac{1}{w\omega_1' g Q_u} \tag{32}$$

and where g is the value of any element between g_1 and g_n. A normalized frequency variable v can also be defined

$$v = \frac{1}{\omega' g}\,. \tag{33}$$

Defining a complex variable $X=u-jv$ permits us to express the matrices of (30) and (31) as

$$\begin{bmatrix}1 & 0\\ \dfrac{1}{X} & 1\end{bmatrix} \tag{34}$$

$$\begin{bmatrix}1 & \dfrac{1}{X}\\ 0 & 1\end{bmatrix} \tag{35}$$

respectively. This indicates that the filter responses are functions of a single complex variable X. The matrix of a single shunt and series combination is the product of the foregoing matrices and is

$$\begin{bmatrix}1 & \dfrac{1}{X}\\ \dfrac{1}{X} & 1+\dfrac{1}{X^2}\end{bmatrix}. \tag{36}$$

This is multiplied by $n/2$ alike matrices (for n even) to determine the overall matrix. For n odd, we multiply $(n-1)/2$ alike matrices and multiply this result by (34). Using matrix expansion formulas contained in Taub [4] and Storch [9] gives the following result:

$$L = 10\log\frac{|M_n|^2}{4}\ \text{dB} \tag{37}$$

where

$$|M_1|^2 = \left|2+\frac{1}{X}\right|^2$$

$$|M_2|^2 = \left|2+\frac{2}{X}+\frac{1}{X^2}\right|^2$$

$$|M_3|^2 = \left|2+\frac{3}{X}+\frac{2}{X^2}+\frac{1}{X^3}\right|^2$$

$$|M_4|^2 = \left|2+\frac{4}{X}+\frac{4}{X^2}+\frac{2}{X^3}+\frac{1}{X^4}\right|^2$$

$$|M_5|^2 = \left|2+\frac{5}{X}+\frac{6}{X^2}+\frac{5}{X^3}+\frac{2}{X^4}+\frac{1}{X^5}\right|^2$$

$$|M_6|^2 = \left|2+\frac{6}{X}+\frac{9}{X^2}+\frac{8}{X^3}+\frac{6}{X^4}+\frac{2}{X^5}+\frac{1}{X^6}\right|^2$$

$$|M_7|^2 = \left|2+\frac{7}{X}+\frac{12}{X^2}+\frac{14}{X^3}+\frac{10}{X^4}+\frac{7}{X^5}+\frac{2}{X^6}+\frac{1}{X^7}\right|^2$$

$$|M_8|^2 = \left|2+\frac{8}{X}+\frac{16}{X^2}+\frac{20}{X^3}+\frac{20}{X^4}+\frac{12}{X^5}+\frac{8}{X^6}+\frac{2}{X^7}+\frac{1}{X^8}\right|^2.$$

These expressions are identical to those for the lossy equal-element band-pass filter, as given in (B-9) of reference [4], except that $1/X$ replaces the X used in the band-pass case.

Expressions for any value of n can be determined in a manner similar to that given in (B-11) of reference [4]. The result for the band-stop case is

$$|M_n|^2 = \left| \sum \left[\binom{n-s}{s} \frac{1}{X^{n-2s}} + \binom{n-2-s}{s} \frac{1}{X^{n-2-2s}} + 2\binom{n-1-s}{s} \frac{1}{X^{n-1-2s}} \right] \right|^2$$

where the summation of s includes only terms where $n-2s$, $n-2-2s$, $n-1-2s$ are all equal to, or greater than, zero. The terms within the parentheses are binomial coefficients, tables of which have been compiled by the Smithsonian Institute [10].

ACKNOWLEDGMENT

The authors are grateful to V. Lee of Airborne Instruments Laboratory, Cutler-Hammer, Inc., for having performed the numerical calculations.

REFERENCES

[1] L. Young, G. L. Matthaei, and E. M. T. Jones, "Microwave band-stop filters with narrow stop bands," *IRE Trans. on Microwave Theory and Techniques*, vol. MTT-10, pp. 416–427, November 1962.
[2] B. M. Schiffman and G. L. Matthaei, "Exact design of band-stop microwave filters," *IEEE Trans. on Microwave Theory and Techniques*, vol. MTT-12, pp. 6–15, January 1964.
[3] S. B. Cohn, "Dissipation loss in multiple-coupled resonator filters," *Proc. IRE*, vol. 47, pp. 1342–1348, August 1959.
[4] J. J. Taub, "Design of minimum loss band-pass filters," *Microwave J.*, vol. 6, pp. 67–76, November 1963.
[5] L. Young, "Group delay and dissipation loss in transmission-line filters," *IEEE Trans. on Microwave Theory and Techniques (Correspondence)*, vol. MTT-11, pp. 215–217; May 1963.
[6] H. A. Bethe, "Lumped constants for small irises," MIT Radiation Labs., Cambridge, Mass., Rept. 43-22, March 1943.
[7] S. B. Cohn, "Determination of aperture parameters by electrolytic-tank measurements," *Proc. IRE*, vol. 39, pp. 1416–1421, November 1951.
[8] S. B. Cohn, "Microwave coupling by large apertures," *Proc. IRE*, vol. 40, pp. 696–699, June 1952.
[9] L. Storch, "The transmission matrix of N alike cascaded networks," *Trans. AIEE (Communications and Electronics)*, vol. 73, pp. 616–618, 1954 (January 1955 Sect.)
[10] *Smithsonian Mathematical Formulae and Tables of Elliptic Functions.* Washington, D. C.: Smithsonian Institute, 1922, p. 20.

YIG Filters as Envelope Limiters

R. C. CUMMING, SENIOR MEMBER, IEEE, AND D. W. HOWELL, STUDENT MEMBER, IEEE

Abstract—Envelope limiters are used in such applications as FM demodulation and power leveling. Recently, the envelope-limiting properties of yttrium-iron-garnet (YIG) filters were reported for the special cases of unmodulated and pulsed input signals. Measured data is presented here on the response of a YIG limiter to AM carriers having modulation index of the order of 50 percent. Sinusoidal, square-wave, and low-pass noise modulating signals were used in the measurements. It was found that a YIG filter will give good envelope limiting for modulating frequencies in the submegacycle range. At these low frequencies the carrier and the side frequencies are not limited selectively. At higher modulating frequencies where the limiting is frequency selective, the YIG filter will not remove the envelope variations. In fact, in the particular filter tested, the modulation index was increased, rather than decreased, at modulating frequencies greater than about 750 kc/s. A graph is given showing the measured factor of reduction (or increase) of modulation index, as a function of modulating frequency. The response of the limiter as a function of carrier frequency, modulating frequency, and input power is shown by oscilloscope displays produced by sweeping the carrier frequency or input power. In addition, selected photographs of output envelope waveforms are given.

Manuscript received April 1, 1965; revised June 4, 1965. This paper is based on work sponsored by the Air Force Avionics Lab., Wright-Patterson Air Force Base, Ohio, under Contract AF 33(657)-11144.
The authors are with Electronics Laboratories, Stanford University, Stanford, Calif.

INTRODUCTION

THE APPLICATION of a YIG filter as a conventional bandpass limiter, i.e., the kind of limiter that removes envelope variations from a narrowband signal, is presented. This *envelope limiter* should be distinguished from the frequency-selective type where each frequency component in the signal is limited independently [1], [2]. Perhaps the most familiar application of envelope limiters is in FM demodulators, where they are used to prevent envelope variations from appearing in the output. Another application is in power leveling of signal generators.

The general conclusion of our work is that a YIG filter will function as an envelope limiter for relatively slow envelope variations, and as a frequency-selective limiter for relatively fast envelope variations. In terms of sinusoidal amplitude modulation, when the modulating frequency is low relative to the decay time constant of the spin-wave modes of the YIG, the filter acts as an envelope limiter. When the modulating frequency is high relative to that time constant, the device acts as a frequency-selective limiter.

The envelope-limiting properties of YIG filters have